European Polymer Journal 114 (2019) 485–500

Contents lists available at ScienceDirect

European Polymer Journal

journal homepage: www.elsevier.com/locate/europolj

Evaluation of commercially available styrene-co-maleic acid polymers for the extraction of membrane proteins from spinach chloroplast thylakoids

Olena Korotych[a,b,*], Jyotirmoy Mondal[a], Kerim M. Gattás-Asfura[c], Jessica Hendricks[a], Barry D. Bruce[a,d,*]

[a] Department of Biochemistry, and Cellular, and Molecular Biology, University of Tennessee at Knoxville, 1311 Cumberland Avenue, Knoxville, TN 37996-1939, United States
[b] Department of Chemical Engineering, University of Florida, 1030 Center Drive, Gainesville, FL 32611-6131, United States
[c] Department of Biomedical Engineering, University of Florida, 1275 Center Drive, Gainesville, FL 32611-6131, United States
[d] Department of Microbiology, University of Tennessee at Knoxville, 1311 Cumberland Avenue, Knoxville, TN 37996-1937, United States

ARTICLE INFO

Keywords:
styrene-co-maleic acid lipid particle (SMALP)
styrene-maleic acid (SMA) copolymer
poly(styrene-co-maleic acid) salt (pSMA-S)
membrane protein
thylakoid
solubilization efficacy

ABSTRACT

Solubilization of membrane proteins by poly(styrene-co-maleic acid) salts (pSMA-S) has significant potential for membrane protein studies. This approach provides an opportunity to overcome many disadvantages associated with a traditional detergent-based technique including protein denaturation and displacement of boundary lipids which may offer both structural and functional stability to membrane proteins. Thylakoid membranes (TMs) from photosynthetic organisms are well studied protein-rich membranes that host several multi-subunit protein complexes associated with oxygenic photosynthesis. These protein complexes are important for applied photosynthesis and by being extracted and purified they can be used in the near future for direct energy conversion. In this study, we used spinach TMs isolated from purified intact chloroplasts to systematically test the solubilization efficacy of 12 commercially available styrene-maleic acid (SMA) copolymers that vary in size, styrene-to-maleic acid molar ratio, and type of ester group. The efficacy of these pSMA-S to solubilize protein-containing biomembranes was evaluated via quantification of protein and chlorophyll content in the resulting SMA Lipid Particles (SMALPs). In addition, the extracted polymer-lipid-protein complexes were studied by low temperature fluorescence, sodium dodecyl sulfate and clear native polyacrylamide gel electrophoresis (SDS- and CN-PAGE), and immunoblot analysis. Our results indicate considerable variability in the solubilization efficacy of commercially available pSMA-S with at least 5 polymer formulations being able to efficiently extract membrane proteins from TMs. These 5 SMA copolymers may also be effective in extraction of membrane proteins from other biomembranes.

1. Introduction

Poly(styrene-co-maleic anhydride) (pSMAnh) is a polymer that is synthesized from styrene and maleic anhydride monomers and can be converted into water-soluble substances such as salts and esters through alkaline hydrolysis and esterification, respectively, (Fig. 1) or via chemical modification, for example, yielding poly(styrene-co-maleimide quaternary ammonium) [1]. Salts of SMA copolymers, poly (styrene-co-maleic acid) salts (pSMA-S), represent a class of substances known as polymeric surfactants which have been used as emulsifying and dispersing agents for at least half a century [2], and just a decade ago researchers started to utilize these polymers for solubilization of

Abbreviations: APS, ammonium persulfate; ATPase, adenosine triphosphatase; ATR, attenuated total reflection; BCA, bicinchoninic acid; BSA, bovine serum albumin; CAB, chlorophyll *a/b* binding; CBB, coomassie brilliant blue; CN-PAGE, clear native – polyacrylamide gel electrophoresis; DMF, dimethylformamide; DDM, n-dodecyl-*β*-D-maltoside; DTT, dithiothreitol; EDTA, ethylenediaminetetraacetic acid; FTIR, Fourier transform infrared; IF, insoluble fraction; HRP, horseradish peroxidase; LHC, light-harvesting complex; LT, low temperature; NIST, the National Institute of Standards and Technology; PS, photosystem; pSMAnh, poly(styrene-co-maleic anhydride); pSMA-S, poly(styrene-co-maleic acid) salt; s/m ratio, styrene-to-maleic acid molar ratio; SDS-PAGE, sodium dodecyl sulfate – polyacrylamide gel electrophoresis; SE, solubilization efficacy; SF, soluble fraction; SI, supportive information; SMA, styrene-co-maleic acid; SMALP, styrene-co-maleic acid lipid particle; TEMED, tetramethylethylenediamine, N, N, N', N'-; TM, thylakoid membrane; UV, ultraviolet

* Corresponding authors at: Department of Biochemistry, and Cellular, and Molecular Biology, University of Tennessee at Knoxville, 1311 Cumberland Avenue, Knoxville, TN 37996-1937, United States.
E-mail addresses: o.i.korotych@gmail.com (O. Korotych), bbruce@utk.edu (B.D. Bruce).

https://doi.org/10.1016/j.eurpolymj.2018.10.035
Received 26 June 2018; Received in revised form 17 October 2018; Accepted 22 October 2018
Available online 23 October 2018
0014-3057/

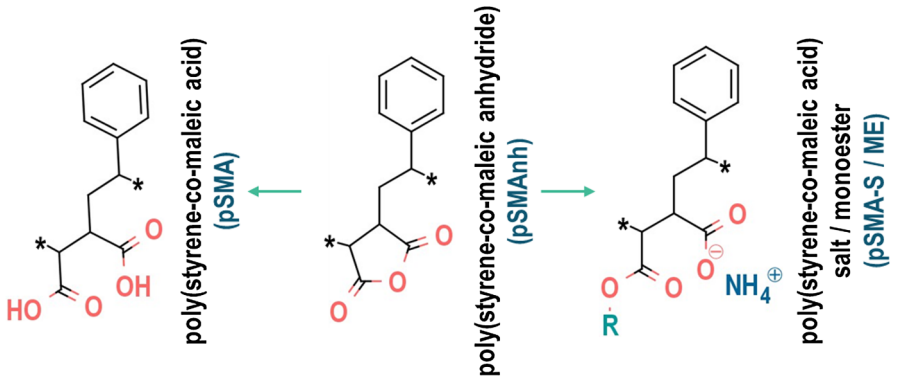

Fig. 1. Chemical structures of poly(styrene-co-maleic acid) derivatives with styrene-to-maleic molar ratio 1:1.

synthetic lipids [3–7] and native biomembranes [8–11]. This approach provides a new opportunity to isolate and characterize multi-subunit membrane protein complexes and supramolecular complexes in their native form and lipid environment [12,13]. In addition, this method can be compatible with a wide variety of biophysical and analytical techniques which are widely employed for structural and functional characterization of extracted membrane proteins [12,14]. This makes membrane protein extraction with pSMA-S an attractive alternative to the traditional detergent-based method [12,15] and *may provide a cost-effective process* for isolating polymer-lipid-protein complexes, which are referred to as protein-containing styrene-co-maleic acid lipid particles (SMALPs). Aside from potential applications of SMA copolymers in membrane protein research, they have already found many applications in cosmetic production and in pharmaceutical industry for preparation of stable oil-in-water emulsions [5], stabilization of different active ingredients such as ascorbic acid and its derivatives, or preparation of conjugates to the antitumor agent neocarcinostatin [5]. Poly(styrene-co-maleic acid) derivatives also can be used to develop pharmaceutical nanotechnology for targeted delivery of drugs and genetic materials [3,4].

A number of publications have shown that pSMA-S with relatively small M_w (less than 10 kDa) and with a styrene-to-maleic acid molar ratio (s/m ratio) 2:1 and 3:1 have been effective in lipid solubilization and membrane protein extraction [13,16,17]. It has also been shown that solubilization of synthetic lipid membranes by a SMA copolymer with s/m ratio 3:1 is not defined by properties of the individual lipids, but rather depends on the properties of the membrane or membrane domains in which these lipids reside [18]. Thus, lipid packing can affect the penetration of SMA copolymers into the lipid membrane and impair its solubilization [6,15]. At the same time, the correlation between protein properties (e.g., size, shape, net charge) and their ability to be extracted by SMA copolymers remains controversial and unresolved. A few researchers have suggested that membrane protein extraction is strongly influenced by the molecular weight of target proteins [9], yet some reports have not found any protein size dependence [19]. There has also been a computational approach that suggests the maximum number of transmembrane domains that can be stably captured and maintained within a SMALP is between 34 and 40 [20]. For this calculation, the authors used the lower size limit currently known for SMALPs, which is equal to 10 nm in diameter. Given that the size of the lipid nanodiscs is inversely proportional to the concentration of the copolymer, we expect that the final size of protein-containing SMALPs will be more likely to depend on the size of the protein itself. Yet some researchers, for example, Lee et al. [8], using the aforementioned computational result have concluded that only proteins less than 400 kDa can be successfully solubilized by SMA copolymers, even though the number of α-helices is not directly proportional to the molecular weight of proteins.

Dr. Barry Bruce's research group (University of Tennessee at Knoxville) has successfully isolated cyanobacterial photosystem I (PSI) trimeric complex with a molecular mass of ~ 1.2 MDa using SMA copolymer [21]. Other researchers have reported on the isolation of a large PSI – light-harvesting chlorophyll II supramolecular complex by SMA copolymer as well [9]. These experimental results suggest that the size range of membrane proteins which can be extracted with SMA derivatives may extend well above 1 MDa, yet this may need to be systematically tested.

The pH-sensitivity of copolymers and interference of divalent cations with SMALP formation/stability is supported by several reports [1,12,13,16,19,22–25]. The observation that a pH approximately less than 7–8 and divalent cations (starting at approximately 5 mM) cause copolymer precipitation can indicate limitation of pSMA-S technology. But this limitation can be overcome by working within a defined pH range, removing free divalent cations by washing with chelating agents such as ethylenediaminetetraacetic acid (EDTA), or through extensive prewashing of the membranes before solubilization with buffers free of divalent cations.

Commercially available SMA copolymers which have many industrial applications [23] provide advantages over polymers synthesized in the laboratory due to their convenience, quality assurance, reproducibility, and accessibility to many researchers around the world. However, the availability of different pSMA-S with wide-ranging s/m ratios and highly variable molecular weights offers many potential polymers for experimental use in the laboratory. Thus, having SMA copolymer systematically characterized for membrane protein extraction will enable scientist to choose a polymer type for their research deliberately. Since the way scientists determine solubilization efficacy (SE) varies between different laboratories, it is crucial for a wide variety of pSMA-S to be tested in one laboratory to provide an accurate and direct comparison. Additionally, identifying the SMA copolymer properties responsible for their high solubilization efficacy will allow to further advance the polymer surfactant technology.

Recent progress in applied photosynthesis demonstrates the ability to use isolated photosystems I from plants and cyanobacteria for direct solar energy conversion to provide either direct photocurrents [26,27] or to form molecular H_2 [28,29]. Applied photosynthesis may greatly benefit from the much lower cost of solubilization and potentially increased stability of complexes that pSMA-S technology may offer. Therefore, we decided to explore the potential role of protein-containing SMALPs for applied photosynthesis while performing systematical testing of twelve pSMA-S with s/m ratio between 1 and 3 comparing their ability to solubilize membrane proteins from higher plant thylakoid membranes. As it is well-known, thylakoids form a dynamic network of two interconnected membrane domains: a region of multiple oppressed or stacked membranes known as grana that is contiguous with a more extended unstacked region known as the stromal lamellae. In this study we used thylakoids isolated from intact spinach chloroplasts as a model biomembrane for testing multiple commercially

available pSMA-S that vary in chemical composition, size, and s/m ratio. Correlations between physical properties (s/m ratio, molecular weight, and dispersity) of polymers and their solubilization efficacy were analyzed using Pearson's product moment and Spearman's Rank correlation coefficients. Such methods as UV–visible spectroscopy, FTIR spectroscopy, low temperature (77 K) fluorescence, sodium dodecyl sulfate and clear native polyacrylamide gel electrophoresis (SDS- and CN-PAGE) were used to characterize the membrane proteins, pSMA-S, and/or their complexes.

2. Materials and methods

2.1. Materials

Acetic acid (Fisher Chemical, A38-12); **Acetone** (Fisher Scientific, A949); **Agarose quick dissolve LE** (Apex™ BioResearch Products, Genesee Scientific, 20-101); **Albumin standard** (Pierce, 23209); **Ammonium hydroxide** (Mallinckrodt, 3256); **Ammonium persulfate (APS)** (Fisher BioReagent, BP179); **L(+)-ascorbic acid, sodium salt** (Fluka, BioChemica, 11140); **Blue dextran** (Sigma, D5751); **Bovine serum albumin (BSA) fraction V** (United States Biochemical, 70195); **Bromophenol Blue** (BioRad Laboratories, 161-0404); **Coomassie Brilliant Blue G-250 (CBB G-250)** (Sigma, B-1131); **Coomassie Brilliant Blue R-250 (CBB R-250)** (Fisher BioTech, BP101); **n-Dodecyl-β-D-maltoside (DDM)** (AdipoGen®, Life Sciences, AG-CC1-0004); **Dry milk (instant), non-fat** (Kroger); **DL-dithiothreitol (DTT)** (Gold Biotechnology, Inc., DTT100); **4-(2-Hydroxyethyl)-1-piperazinepropanesulfonic acid (EPPS or HEPPS)** (Sigma, E9502); **N,N,N',N'-Ethylenediaminetetraacetic acid, tetrasodium salt, dihydrate ($C_{10}H_{12}N_2O_8Na_4{\cdot}2H_2O$)** (United States Biochemical, 15700); **L-Glutathione reduced** (Sigma, G4251); **Glycerol** (Fisher Bioreagent, BP229); **Glycine (aminoacetic acid)** (National Diagnostics, EC-405); **4-(2-Hydroxyethyl)-1-piperazineethanesulfonic acid (HEPES)** (Fisher Chemical, BP310); **Hydrochloric acid** (Fisher Scientific, A142); **Magnesium chloride, anhydrous** (Acros Organics, 223210010); **Manganese chloride, tetrahydrate** (Fisher Scientific, M–87); **Methanol** (Sigma-Aldrich, 179337); **Peirce® BCA Protein Assay Reagent A** (Thermo Scientific, 23223); **Peirce® BCA Protein Assay Reagent B** (Thermo Scientific, 23224); **Percoll™** (GE Healthcare, 17–0891-09); **polyoxyethylene-20-sorbitol monolaurate (Tween® 20)** (Fisher BioRegents, Fisher Chemicals, BP337); **Potassium chloride** (Fisher Chemical, P217); **Potassium hydroxide** (Fisher Scientific, P250); **ProtoGel** (30% (w/v) acrylamide and 0.8% (w/v) N,N'-bisacrylamide stock solution, 37.5:1) (National Diagnostic, EC-890); **Sodium bromide, anhydrous** (Sigma-Aldrich, 746401); **Sodium carbonate, anhydrous** (Fisher Scientific, BP 357); **Sodium dodecyl sulfate (SDS)** (Fisher Biotech, BP166); **D-sorbitol** (Fischer Scientific, S459); **Sypro® Ruby protein gel stain** (Molecular probes, S12001); **N,N,N',N'-tetramethylethylenediamine (TEMED)** (Fischer BioReagents, BP150); **Trichloroacetic acid** (Sigma, T-6399); **N-[Tris (hydroxymethyl)methyl] glycine (Tricine)** (Bioland Scientific LLC, CT03); **Tris base** (Amresco, 0497); **Triton X-100** (Fisher BioReagent, BP-151-500).

All reagents were used as received without further purification. Water purified by Milli-Q® Q-Gard® 2 (Millipore Sigma) and denoted as DI H_2O was used as a solvent in all experiments.

2.2. Hydrolysis of poly(styrene-co-maleic) acid anhydrides

Commercially available polymers are available in both forms: anhydrides and salts. A few polymers, namely SMA® PRO 10235 and Lustran® 245 NR, were supplied as anhydrides only and have been converted to ammonium salts by refluxing the polymers with constant stirring in the presence of ammonium hydroxide at 75 °C for 5 h and at 95 °C for 20 h, respectively. The amount of hydroxide solution (29.4 wt %) was estimated according to the Cray Valley APPLICATION BULLETIN "Solubilizing SMA® resins in water" using the following formula:

$$m\ \ (hydroxide\ \ solution) = \frac{M\,(hydroxide){\bullet}AN{\bullet}m\,(anhydride){\bullet}EF}{56,\,100{\bullet}w\ \ (hydroxide)} \quad (1)$$

where $m(hydroxide\ \ solution)$ – amount of hydroxide solution required for hydrolysis [g];
$M(hydroxide)$ – molar mass of hydroxide [Da];
AN – acid number of polymer [mg of KOH/1 g of anhydride];
$m(anhydride)$ – the mass of poly(styrene-co-maleic acid) anhydride being hydrolyzed [g];
EF – excess factor[1] [a.u.];
$w(hydroxide)$ – concentration of aqueous hydroxide solution [wt.%].

First, solid styrene-maleic acid anhydride was mixed with DI H_2O (75% of final volume). Then, the calculated amount of hydroxide solution from Eq. (1) was added gradually over the time to the anhydride keeping the pH constant around 8.5–9.5 until the polymer was completely dissolved. After the completion of hydrolysis, the final concentration of SMA copolymer in solutions was adjusted with DI H_2O to 20 and 10 wt% for SMA® PRO 10235 and Lustran® 245 NR, respectively. The hydrolyzed polymer solutions were stored at room temperature away from direct sun.

2.3. Isolation of intact chloroplasts from Spinacia oleracea

Intact chloroplasts were isolated from market spinach (*Spinacia oleracea*) leaves using a method adapted from Bruce et al. [30]. Spinach leaves were washed in cold water, dried with filter paper, and cut into 0.5–1.0 cm pieces using scissors. The leaves were homogenized in ice-cold grinding buffer (GB) (50 mM HEPES-KOH with pH 7.3, 330 mM sorbitol, 0.1% (w/v) bovine serum albumin (fraction V), 1 mM $MnCl_2$, 1 mM $MgCl_2$, and 2 mM EDTA tetrasodium salt) with an approximate ratio of 200 mL of buffer for every 100 g of fresh leaves. A small amount of sodium ascorbate and reduced glutathione were added to the buffer before homogenization. Spinach leaves were ground in a Polytron homogenizer PT 90/35 (Brinkman Laboratories) with a 12 mm diameter probe at maximum speed by three pulses (a few seconds long). The homogenate was filtered through two layers of Miracloth (Calbiochem, 475855) and two layers of cheesecloth into an Erlenmeyer flask submerged in ice and centrifuged using a Sorvall RC 6+ centrifuge (Thermo Scientific) and F10-6 × 500y rotor (FiberLite™, Piramoon Technologies) at 2500*g* for 15 min to pellet the chloroplasts. After centrifugation, the supernatant was carefully decanted without disturbing the pellet and discarded. In order to reduce the cytoplasmic contamination, the chloroplast pellet was washed twice by resuspending in GB (50% of the original volume) and repeating the previous centrifugation step. After last wash step, the chloroplast pellet was resuspended in import buffer (IB) (50 mM HEPES-KOH with pH 8.0, 330 mM sorbitol) (10% of the previous volume) and carefully overlaid on top of the ice-cold Percoll™ gradient in IB with 80 vol% cushion and 40 vol% top layer. The gradients with overlaid samples were spun in an F15-8 × 50C rotor (FiberLite™, Piramoon Technologies) at 3,600*g* for 15 min with an intermediate brake. The crude chloroplasts were resolved into two bands: an upper one, resting above the 40% Percoll™ gradient, which consisted of a mixture of broken chloroplasts and thylakoid membranes (TMs), and a lower green band at the 40–80% interface, which consisted of intact spinach chloroplasts. The lower layer of intact chloroplasts was carefully collected. To remove Percoll™ solution from the chloroplasts, the intact chloroplasts

[1] Usually 5 to 15% excess of hydroxide is used in the reaction to speed up the hydrolysis of anhydrides, or, in reactions involving volatile amines (such as ammonium hydroxide), to compensate for vapor loss. In these cases, the excess factor referred to in the Eq. (1) would be 1.05–1.15.

were diluted fourfold with ice-cold IB and pelleted by centrifugation at 2,500*g* for 15 min. The wash step was repeated and then washed chloroplasts were resuspended in IB. Chlorophyll concentration in final chloroplast solution was determined by extraction with aqueous 80 vol % acetone solution (see Section 2.8).

2.4. Isolation of crude thylakoid membranes from Spinacia olaracea

Intact chloroplasts form Section 2.3 were pelleted in an F15-8 × 50C rotor (FiberLite™, Piramoon Technologies) at 2,500 *g* for 15 min and resuspended in equal volume of 0.1 × IB for a mild hypotonic lysis. The sample was incubated on ice at least for 30 min. After the incubation the lysed chloroplasts were split in two separate vials and each sample was centrifuged at 25,000*g* for 15 min to pellet the TMs. The TMs was washed twice with the same volume of 0.1 × IB containing either 5 mM EDTA tetrasodium salt (hereinafter the sample is denoted as EDTA prewashed TMs) or 3 mM $MnCl_2$ and 3 mM $MgCl_2$ (the sample is denoted as Me prewashed TMs) using the previous centrifugation settings. During each resuspension samples were Dounce homogenized using 55 mL glass tissue grinder with Teflon® pestle (Wheaton, 358054). After the last wash the isolated TMs were resuspended in sample buffer (GKSB-150) (50 mM glycine-KOH with pH 8.6, 150 mM KCl and 20 vol% glycerol) or in 1 × IB to yield solutions with concentration of approximately 0.25 mg/mL of chlorophyll, Dounce homogenized, aliquoted, and stored at −20 °C until further usage.

2.5. Removing stromal and peripherally associated proteins from thylakoid membranes

To remove stromal and peripherally associated proteins from the thylakoids, the membranes were washed using three different procedures which consists of treatment of crude TMs with glycine potassium chloride buffer (GKB-150) (50 mM glycine-KOH with pH 8.7, 150 mM KCl), with GKB-150 containing 1 M NaBr (chaotropic agent), or with 100 mM Na_2CO_3 [31]. TMs were diluted at least threefold with aforementioned solutions and incubated on ice for 30 min. The suspensions were vortexed for a few seconds and centrifuged using an Optima MAX Ultracentrifuge (Beckman Coulter) and TLA-55 rotor (Beckman Coulter) at 24,000 rpm (~ 35,000*g*) for 10 min at 4 °C. The membrane pellets were washed twice with ice-cold GKB-150 to remove completely NaBr and Na_2CO_3 and finally resuspended in GKSB-150 of the same volume as the original sample. All supernatants were collected and centrifuged one more time to completely remove TMs. Supernatants (100 µL) were dialyzed for 1 h against glycine buffer without salt (GB-0) (50 mM glycine-KOH with pH 8.9) using Slide-A-Lyzer® mini dialysis units with 10 kDa molecular weight cut-off (Thermo Scientific, 69572). The volume ratio between samples and dialyzing buffer was approximately 1:500. The buffer during dialysis was changed twice (every 30 min). Dialyzed samples were further analyzed using SDS-PAGE (see Section 2.13), the protein bands were visualized by staining overnight with Sypro® Ruby according to the supplier protocol. Protein and chlorophyll content in washed membranes were determined according to the procedures described in Section 2.8 and Section 2.9. Washed TMs were analyzed by SDS-PAGE as well (Section 2.13).

2.6. Thylakoid membrane solubilization trials

Solubilization trials were carried out using crude TMs from Section 2.4 and washed TMs from Section 2.5. Spinach TMs in GKSB-150 containing approximately 2.5 mg/mL of proteins or 0.25 mg/mL of chlorophyll were mixed with equal volume of 5.0 ± 0.2 wt% pSMA-S solution in GKB-150. The final pSMA-S concentration was 2.5 wt%. Additionally, GKB-150 was used as a negative control, while 0.5 wt% n-dodecyl-*β*-D-maltoside (DDM) in GKB-150 was used as a positive control. The solubilization was carried out in the dark at 20 °C or at 40 °C for two hours on the orbital shaker (200 rpm). After 2 h all samples were centrifuged using an Optima MAX Ultracentrifuge (Beckman Coulter) and TLA-55 rotor (Beckman Coulter) at 20,000 rpm (24,640*g*) for 10 min at 4 °C. The supernatant containing SMALPs was carefully aspirated without disturbing the pellet which was resuspended in equal volume of glycine resuspending buffer (GKRB-150) (50 mM glycine-KOH pH 8.5, 150 mM KCl, 10% glycerol). The supernatant was centrifuged one more time to completely remove insoluble membranes from the sample. Both samples containing soluble and insoluble membrane protein fractions (SF and IF) as well as initial sample before centrifugation were analyzed by UV–visible spectroscopy (Section 2.7), low temperature (LT) fluorescence (Section 2.11), and SDS-PAGE (Section 2.13). The total protein concentration was determined using bicinchoninic acid (BCA) assay (Section 2.9), while the total chlorophyll, chlorophyll *a*, and chlorophyll *b* content was determined after its extraction by 80 vol% aqueous acetone solution (Section 2.8).

2.7. UV–vis spectroscopy

UV–vis spectra between 200 nm and 800 nm of samples during solubilization (sample before centrifugation and two fractions after centrifugation: SF and IF) were recorded in a quartz cuvette with a pathlength of 1 cm using double/split beam UV–vis spectrophotometer Evolution™ 300 (Thermo Scientific). All spectra were collected on 500 µL of sample using 1 nm bandwidth and 240 nm/min scanning speed. The original samples were diluted 20 times with GKRB-150 before measurements, unless stated otherwise. Each spectrum was background corrected with the buffer. No further correction for scattered light was needed.

2.8. Chlorophyll extraction and determination

The procedure for chlorophyll determination was based on the Arnon work [32] using spectrophotometric quantification of chlorophylls in aqueous 80 vol% acetone extracts. Briefly, 10 µL of sample was mixed with 990 µL of 80 vol% aqueous acetone solution, vortexed for a few seconds, and centrifuged at 20,000*g* for 1 min using Sorvall legend Micro 21 centrifuge (Thermo Electron Corporation). The absorbance of supernatant was recorded within 30 min at 645 and 663 nm using the same set up as described in Section 2.7. The concentration of total chlorophyll ($C_{total\ \ chl}$), chlorophyll *a* ($C_{chl\ \ a}$), and chlorophyll *b* ($C_{chl\ \ b}$) was calculated using the following formulas:

$$C_{total\ \ chl} = \frac{(20.20 \bullet A_{645} + 8.02 \bullet A_{663})}{1000} \bullet DF, \quad (2)$$

$$C_{chl\ \ a} = \frac{(12.70 \bullet A_{663} - 2.69 \bullet A_{645})}{1000} \bullet DF, \quad (3)$$

$$C_{chl\ \ b} = \frac{(22.90 \bullet A_{645} - 4.68 \bullet A_{663})}{1000} \bullet DF, \quad (4)$$

Where A_{645} and A_{663} is the absorbance of acetone extract at 645 and 663 nm, respectively [a.u.];
DF is the dilution factor [a.u.].

Equations derived by Porra et. al. [33] were used for estimation of chlorophyll content as well and compared with the values obtained from Eqs. (2)–(4) (Table SI).

2.9. Bicinchoninic acid (BCA) assay for protein determination

The Pierce™ bicinchoninic acid (BCA) protein colorimetric assay was used to determine the total protein content in samples according to the manufacturer's microplate protocol. This method is based on the reduction of Cu^{2+} to Cu^{+} by proteins in an alkaline medium (the biuret reaction) and measuring the absorbance of BCA-Cu^{+} complex. The

562 nm absorbance was measured at 25 °C on a Gen5™ microplate reader (BioTek Instruments) using a pathlength correction. The average absorbance of blank was subtracted from the measurements of all other individual standards and unknown sample replicates. The BSA calibration curve was fitted to a quadratic function ($A_{norm} = aC^2 + bC$). The total protein concentration of unknown samples was calculated using the following formula:

$$C = \frac{-b + \sqrt{b^2 - 4a(-A_{norm})}}{2a} \cdot DF \quad (5)$$

Where C is the total protein concentration [μg of protein/mL];
a and b are the fitted parameters of a quadratic function for the calibration curve;
A_{norm} is the pathlength corrected sample absorbance at 562 nm after the subtraction of the average 562 nm absorbance of a blank solution [cm^{-1}].

2.10. Solubilization efficacy determination

Solubilization efficacy [%] of pSMA-S was estimated as a ratio of protein content or total chlorophyll content in soluble fractions (SF) (C_{SF}) to the concentration of proteins and chlorophylls in sample before centrifugation (C_{total}) according to the formula below:

$$SE = \frac{C_{SF}}{C_{total}} 100\%, \quad (6)$$

We also estimated SE based on absorbance by integration of spectra of SF and sample before centrifugation within 300–800 nm wavelength range:

$$SE = \frac{\int_{A_{300}}^{A_{800}} A_i^{SF}}{\int_{A_{300}}^{A_{800}} A_i^{total}} 100\%, \quad (7)$$

where A_i^{SF} and A_i^{total} are the absorbance of soluble fraction and sample before centrifugation at i nm [a.u.].

2.11. Low temperature fluorescence

Fluorescence measurements at −196 °C (77 K) were performed on PTI Quanta Master™ fluorometer from HORIBA Scientific. The sample was excited at 435 nm, and the emission spectra were recorded using Felix GX software (version 4.2.3010) within 600–800 nm wavelength range using 3 nm slit width, 1 nm step, and 0.5 sec integration time. Three spectra of 10 × diluted samples, unless stated otherwise, were recorded and averaged for each sample. All spectra were background corrected and deconvoluted (Fig. S1) in Origin Pro 2018 (version b9.5.0.193).

2.12. Trichloroacetic acid (TCA) precipitation

To remove lipids and polymer from the samples, membrane proteins from soluble fraction were precipitated in 25% (w/v) trichloroacetic (TCA) acid by mixing the equal volume of sample and 50% (w/v) TCA in DI H_2O. After 10 min incubation on ice, proteins were pelleted using an Optima MAX Ultracentrifuge (Beckman Coulter) and TLA-55 rotor (Beckman Coulter) at 15,000 rpm (13,860*g*) for 10 min at 4 °C. The protein pellets were washed two times by vortexing with 10 volumes of ice cold 100% acetone and repeating the previous centrifugation step. The protein pellets were dried in the air for 15–30 min before being resuspended in 5 × reducing buffer (RB) (250 mM Tris-HCl with pH 6.8, 500 mM dithiothreitol (DTT), 10 wt% SDS, 25 vol% glycerol, and 0.025% bromophenol blue) and analyzed by SDS-PAGE (Section 2.13).

2.13. SDS-PAGE

The polypeptide profile of membrane proteins was analyzed by sodium dodecyl sulfate – polyacrylamide gel electrophoresis (SDS-PAGE). Glycine-SDS-PAGE (known also as Laemmli-SDS-PAGE) and tricine–SDS-PAGE based on tris-glycine and tris-tricine buffer systems, respectively, are the commonly used SDS electrophoretic techniques for separating and analyzing proteins [34]. Sharp banding of the protein components (larger than 30 kDa) has been achieved using a discontinuous Laemmli tris-glycine gel system [35] consisting of 3 wt% stacking (1 cm) and 15 wt% separating (6 cm) gel layers with pH 6.8 and 8.8, respectively. Gels were prepared from a stock solution of 30 wt % acrylamide and 0.8 wt% N,N′-methylenebisacrylamide and polymerized by adding a redox system based on TEMED and APS (1:1 molar ratio). Stacking gel was prepared based on 125 mM tris-HCl buffer with pH 6.8, while 375 mM tris-HCl buffer system with pH 8.8 was used for separating (resolving) gel. Both gel layers contained 0.1 wt% SDS. The tris-glycine electrode running buffer with pH 8.8 contained 25 mM tris, 192 mM glycine, and 0.1 wt% SDS.

For separation of proteins with MW less than 30 kDa and for immunoblotting we used discontinuous tricine–SDS-PAGE which consist of 3 wt% stacking (1 cm) and 15 wt% separating (6 cm) gel layers. Gels were prepared the same way as described before but using different buffer systems (see Table SII).

All buffer solutions and Coomassie stain solution were filtered using a vacuum driven disposable bottle top filtration unit with 0.22 μm GP Millipore Express™ PLUS Membrane (Millipore Sigma SCGPT02RE).

Samples dissolved in 5 × reducing buffer were denatured by heating for 10 min at 65 °C. Electrophoresis was carried out in a vertical Mini PROTEAN® Tetra Cell unit (Bio-Rad) with a constant voltage of 75 V for stacking gel and 150 V for resolving gel for glycine-SDS-PAGE and 50 V and 200 V, respectively, for tricine-SDS-PAGE until the bromophenol blue marker reached the bottom of the gel (approximately 2 h).

Mark 12™ unstained protein standard (Invitrogen by Thermo Fisher Scientific, LC5677) was used for determining protein molecular weights in a range of 2.5–250 kDa.

Proteins were visualized directly in the gel by Coomassie staining. After electrophoresis proteins were fixed for 15 min in solution containing 50 vol% of methanol and 10 vol% of acetic acid, washed twice in distilled water for 15 min, and stained for 0.5–1.0 h in CBB stain (approx. 0.1 wt% CBB R-250, 10 vol% methanol, and 10 vol% acetic acid). The gels were distained by diffusion with repeated washing in solution of 10 vol% methanol and 10 vol% acetic acid and imaged using UVP imaging system. Molecular weights of proteins were calculated using software for acquisition and analysis from UVP VisionWorksLS (version 7.1 RC3.38). For Sypro® Ruby staining we used the basic protocols provided by a supplier.

2.14. CN-PAGE

For separation of native polymer-lipid-protein complexes based on their size and charge, nondenaturing continuous clear native (CN) gel electrophoresis was carried out using various polyacrylamide gradient gels (3–9%, 4–12%, and 4–16%). Five buffer systems with pH around 8.5 were tested, including two buffers based on tris described by McLean [36]: tris-EPPS with pH 8.3 (32 mM tris, 30 mM EPPS); tris-boric acid with pH 8.9 (50 mM Tris, 25 mM boric acid); glycine-KOH with pH 8.6 (50 mM glycine); EPPS-KOH with pH 8.4 (50 mM EPPS); and tricine-KOH wit pH 8.5 (25 mM Tricine).

Electrophoresis was carried out using the set up described in Section 2.13 for an hour at 150 V. Proteins within the gel were stained by CBB (see Section 2.13 for details). For visualization of gel gradient, blue dextran was added to a solution with a higher acrylamide concentration before gel casting (Fig. S2).

Table 1
Characteristics of poly(styrene-co-maleic acid) derivatives including styrene-to-maleic acid molar ratio, weight average (M_w) and number average (M_n) molecular weights, and dispersity (Đ) as specified by suppliers.

Supplier	#	Product Name	Derivative	Styrene : Maleic Acid Molar Ratio	M_w [kDa]	M_n [kDa]	Đ (M_w / M_n) [a.u.]
Polyscope Polymers B.V.	1a	XIRAN® SZ 40005	anhydride	1.4 : 1	5.00	1.90	2.63
	1b	XIRAN® SL 40005 S40	Na^+ salt				
	2a	XIRAN® SZ 30010	anhydride	2 : 1	6.50	2.50	2.60
	2b	XIRAN® SL 30010 S30	Na^+ salt				
	3a	XIRAN® SZ 25010	anhydride	3 : 1	9.20	3.20	2.88
	3b	XIRAN® SL 25010 S25	Na^+ salt				
TOTAL Cray Valley	4a	SMA® 1000 flake	anhydride	1 : 1	5.50	2.00	2.75
	4b	SMA® 1000 HNa	Na^+ salt				
	5	SMA® PRO 10235 powder	anhydride	1.5 : 1	7.00	2.90	2.41
	6a	SMA® 1440 flake (batch 1)	anhydride, ester	1.5 : 1	7.00	2.80	2.50
	6b	SMA® 1440 H (batch 1)	NH_4^+ salt, ester				
	6c	SMA® 1440 flake (batch 2)	anhydride, ester				
	6d	SMA® 1440 H (batch 2)	NH_4^+salt, ester				
	7a	SMA® 17352 flake	anhydride, ester	1.7 : 1	7.00	2.80	2.50
	7b	SMA® 17352 powder	anhydride, ester				
	7c	SMA® 17352 H	NH_4^+salt, ester				
	8a	SMA® 2000 flake	anhydride	2 : 1	7.50	3.00	2.50
	8b	SMA® 2000 H	NH_4^+ salt				
	9a	SMA® 2021 flake	anhydride	2 : 1	21.00	12.00	1.75
	9b	SMA® 2021 H	NH_4^+ salt				
	10a	SMA® 2625 flake	anhydride, ester	2 : 1	9.00	3.60	2.50
	10b	SMA® 2625 powder	anhydride, ester				
	10c	SMA® 2625 H	NH_4^+ salt, ester				
	11a	SMA® 3000 flake	anhydride	3 : 1	9.50	3.80	2.50
	11b	SMA® 3000 H (batch 1)	NH_4^+ ammonium salt				
	11c	SMA® 3000 H (batch 2)	NH_4^+ ammonium salt				
INEOS Styrolution America LLC	12	Lustran® 245 NR	NH_4^+ salt	3 : 1	120.00	—	—

2.15. Immunoblot analysis

The proteins resolved by tricine–SDS-PAGE were electroblotted onto a polyvinylidene difluoride (PVDF) Immobilon®-P membrane with 0.45 μm pore size (Millipore Sigma, IPVH00010) in vertical Mini-PROTEAN® II Cell unit with transfer buffer (TB) (25 mM tris, 192 mM glycine). Individual lanes were cut into strips, blocked for an hour with 5% non-fat milk in tris buffer saline (TBST-NFM) (25 mM tris-HCl with pH 8, 137 mM NaCl, 3 mM KCl, 0.1 vol% Tween-20, 5 wt% non-fat milk) and probed with 9 different primary antibodies overnight. All antibodies were added in 1 : 5000 dilution in TBST-NFM. Membrane with primary antibodies was incubated overnight at 4 °C. The following rabbit polyclonal antibodies were used to probe for the major membrane complexes in thylakoids: α-Subunit IV (b_6/f complex), α-CAB, α-cyt b_6, α-CF_1 (α-subunit), α-CF_1 (γ-subunit), α-PsaC, α-PsbA, α-LHCII, and α-RuBisCO (L-subunit). Before adding a secondary antibody, the membrane was washed three times with TBS-T (25 mM tris-HCl with pH 8, 137 mM NaCl, 3 mM KCl, 0.1 vol% Tween-20). An anti-rabbit horseradish peroxidase (HRP) conjugate secondary substrate in TBST-NFM (1:15,000 dilution) was added and incubated for 45 min at room temperature. The membrane was then washed once with TBST-NFM, followed by TBS-T and TBS (25 mM tris-HCl with pH 8, 137 mM NaCl, 3 mM KCl) for 15 min each. The conjugates were detected using a chemiluminescent HRP substrate. Photos were captured using a Universal hood II (Bio-Rad) and analyzed with a Quantity One software (version 4.5.1.059).

2.16. FTIR spectroscopy

The Fourier transform infrared (FTIR) spectral analysis of functional groups of poly(styrene-co-maleic acid) anhydrides and their hydrolyzed form after lyophilization was carried out on a Frontier FT-IR spectrometer (Perkin Elmer) with PerkinElmer Spectrum software (version 10.4.2.279). The spectra of copolymers were recorded using an attenuated total reflection (ATR) technique in the spectral range 650–4000 cm^{-1} with a resolution of 2 cm^{-1} and accumulations of 10 scans which were combined to average out random absorption artifacts. The spectrometer was equipped with desiccated Ge-coated KBr optics, a temperature-stabilized deuterated triglycine sulfate detector, and 1 reflection diamond/ZnSe universal ATR sampling accessory. Spectra of

polystyrene (transmittance) was recorded and used as a reference for band assignments. Additionally, 2-bromosuccinic anhydride and succinic acid were used as reference substances. Their spectra were obtained from NIST Standard Reference Database 69: NIST Chemistry WebBook [37,38].

2.17. Data analysis and visualization

All data is presented as an arithmetic mean ± standard uncertainty. Standard uncertainty was estimated as following with the systematic error assumed to be negligible:

$$Std.\ uncert = \sqrt{\left(\frac{s}{\sqrt{N}} t_{p,df}\right)^2 + (\Delta y)^2} \quad (8)$$

Where s is the sample standard deviation;
N is the number of parallel experiments;
$t_{\alpha,df}$ is the critical value of two-tailed t-distribution for fraction $p = 68.27\%$with defined degrees of freedom ($df = N - 1$);
Δy is the error of indirect measurements, which was calculated using the numerical differentiation method [39].

Differences between groups were examined for statistical significance using two-tailed t-test with a significance level $\alpha = 0.05$.

To evaluate correlations between solubilization efficacy and physical properties of copolymers, the Pearson's product-moment correlation coefficient and Spearman's rank correlation coefficient were calculated.

All calculations were performed using Microsoft® Excel® 2016 (Microsoft), while OriginPro (Ver. b9.5.0.193, Origin Lab) was used for plotting graphs, curve integration, analyzing and deconvoluting peaks, nonlinear and linear fitting, calculation correlation coefficients, statistical analysis, and graphical residual analysis.

MarvinSketch (version 17.4.3, 2017; ChemAxon) was used for drawing and displaying chemical structures.

3. Results and discussion

3.1. Overview of SMA copolymer properties

The overall goal of the study was to evaluate the efficacy of commercially available pSMA-S listed in Table 1 in extraction of membrane proteins from spinach thylakoids as a function of the polymer physicochemical properties. The concentration of commercially available polymer solutions with s/m ratio ranging from 1 to 3 varies from approximately 15–40 wt% and it agrees (within 5%) with the concentration determined using lyophilization technique. The information on polymer lot numbers and dry content of SMA copolymer solutions can be found in SI (Table SIII and Fig. S3).

In this comparative study we tested twelve commercially available polymers with s/m ratio from 1 to 3 (Table 1). Our study includes different synthetic lots (SMA® 1440 and SMA® 3000) and allows direct comparison of the top-3 most widely used SMA copolymers cited in recent papers – *XIRAN® 25010*, *SMA® 2000*, and *XIRAN® 30010* [6,7,9,10,14,17,19,40–49]. We also tested several SMA polymers for membrane solubilization that have not been reported in the literature, such as *PRO 10235*, *1440*, *17352*, *2021*, and *2625* from TOTAL Cray Valley. The complete list of pSMA-S which are widely used by other researchers for lipid and membrane protein solubilization can be found in Table S IV. Unfortunately, we were unable to include other XIRAN® polymers available from Polyscope Polymers B.V. or the Lipodisq® products from Malvern Cosmeceutics Ltd. due to either their limited availability and generally prohibitively high cost, respectively, but two other comprehensive studies by Morrison et al. [19] and Swainsbury et al. [17] tested eleven and eight commercially available SMA copolymers. Our work is complementary and can be integrated to provide a more complete evaluation of different SMA copolymers. For ease of comparison with the aforementioned studies we kept the same final concentration of pSMA-S equal to 2.5 wt%, even though no concentration dependence was reported in previously published studies.

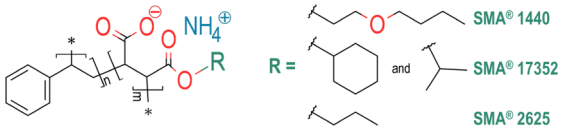

Fig. 2. Chemical structure of partial monoesters of poly(styrene-co-maleic acid) ammonium salts.

SMA copolymers used for this study vary in size from 5.0 to 9.5 kDa and also includes two polymers with weight average molecular weight (hereinafter molecular weight) of 21 and 120 kDa. Besides poly (styrene-co-maleic acid) salts we also evaluated *three partial monoesters* whose structures are depicted in Fig. 2: *SMA® 1440*, *SMA® 17352*, and *SMA® 2625* (Table 1, cells highlighted in darker green).

3.2. FTIR analysis of SMA copolymers

Details about chemical structure of polymer anhydrides and their hydrolyzed forms were obtained from FTIR spectra. Bands related to the styrene moieties were assigned on the basis of the polystyrene (PS) spectrum [50], while bands related to the maleic moieties were assigned based on the spectra of 2-bromosuccinic anhydride and succinic acid.

Based on analogy with the spectra of simple molecules and calculated characteristic frequencies of various molecular groups, the presence of aromatic groups in SMA copolymers can be shown by absorbance bands centered at 3027 cm^{-1} (aromatic C—H stretches) and in the 1500–1600 cm^{-1} region (aromatic C—C stretches) (Fig. 3a–c). A substitution pattern can be identified from absorbance below 900 cm^{-1}, which is caused by out-of-plane bending of the ring C—H bonds. The occurrence of two strong bands in 600–800 cm^{-1} region centered at 699 and 761 cm^{-1} corresponds to monosubstituted derivatives (Fig. 4), as expected. The group of 5 bands in the 1600–2000 cm^{-1} region corresponds to the overtone of aromatic δCH (out-of-plane) and combination tone bands, and it can be observed only for PS and are probably hidden in polymer spectra by strong bands corresponding to C=O absorbance. Weak but sharp bands within the 950–1250 cm^{-1} region can be assigned to in-plane bending of phenyl hydrogen atoms, but they are of secondary importance, given that C—C, C—O, and other single bonds absorb in the same region as well [51]. Bands at 1494, 1602, and 1584 cm^{-1} were assigned to absorbance of the phenyl group (Figs. 3a–c, 4, and 5). The presence of band at 1580 cm^{-1} suggests that the phenyl is conjugated with an unsaturated group, while the band centered at 1450 cm^{-1} (corresponding to the phenyl nucleus) was not resolved due to overlapping with CH_2 band.

Bands corresponding to characteristic vibrations of sp^3-hybridized C—H bonds (methyl and methylene groups) can be found in three regions: 2800–3000, 1300–1400 and below 700 cm^{-1}, and are present in IR spectra of all SMA copolymers and PS. Molecules containing methyl and methylene groups according to theoretical calculations are supposed to have two distinct bands for each group: at 2962 and 2872 cm^{-1} and at 2926 and 2853 cm^{-1}, respectively [52,53]. The first of these two bands results from the asymmetrical (as) stretching, while the second band arises from a symmetrical (s) stretching mode. As one can see in Fig. 3d, bands corresponding to stretching vibrations of methylene groups can be observed only in spectra of SMA® 1440 and SMA® 2625 suggesting their relatively high abundance due to the ester groups in comparison to methylene groups.

Anhydrides display two stretching bands in the carbonyl region resulting from asymmetrical and symmetrical C=O stretching modes. Cyclic anhydrides with five-membered rings show absorbance at higher frequencies. For example, succinic anhydride absorbs at 1789 and

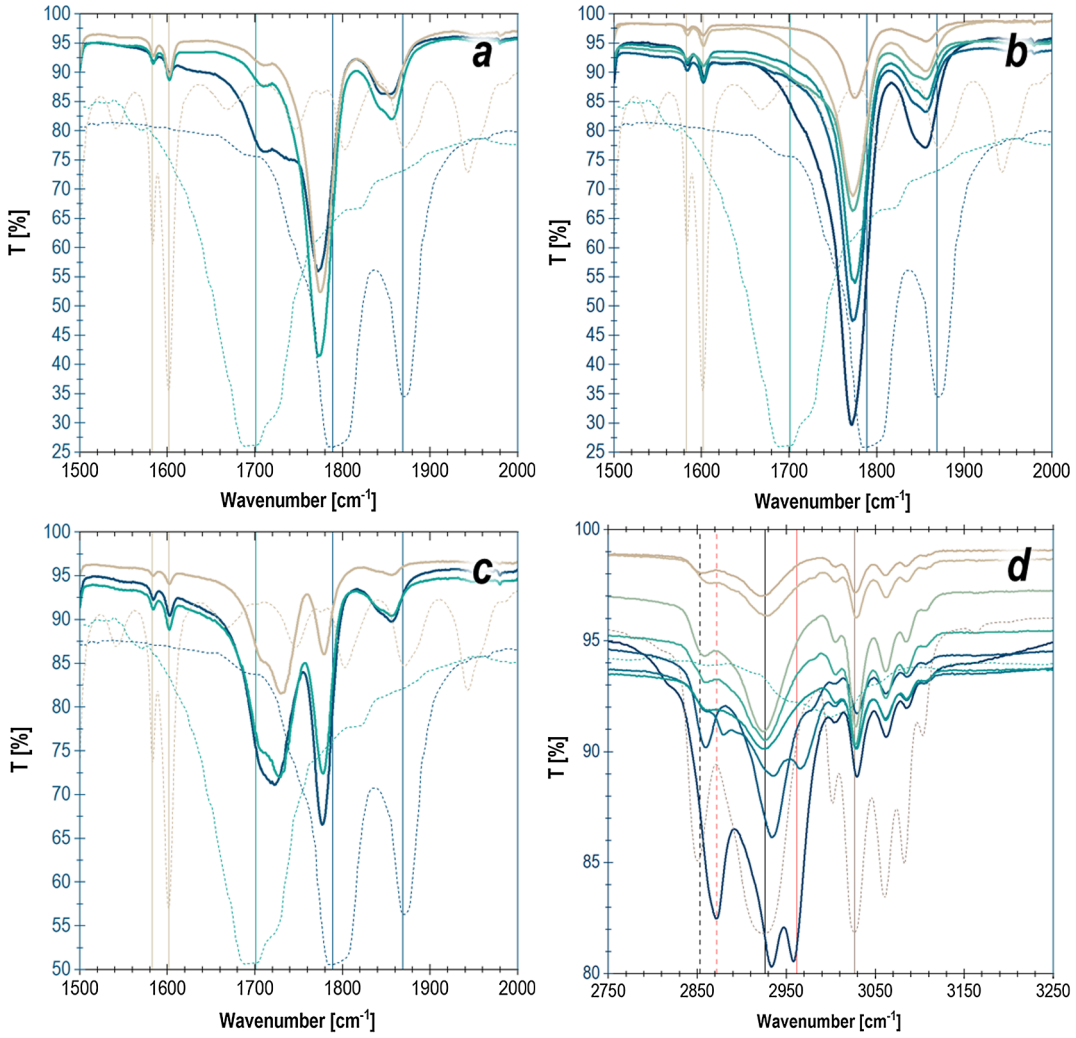

Fig. 3. IR spectra (1500–2000 cm^{-1} region) of poly(styrene-co-maleic anhydrides) (solid lines) and reference substances (dash line): *a* – 40005, 30010, and 25010, *b* – 1000, 2000, 3000, PRO 10235, 2021, and 245 NR; *c* – 17352, 2625, 1440 (lot PS16093002), *d* – 1440 (lot PS14044701), 17352, 2625, 2000, 3000, 25010, 2021, and 245 NR; and 2-bromosuccinic anhydride (blue dash line) with two reference lines at 1789 and 1869 cm^{-1}; succinic acid (green dash line) with 1701 cm^{-1} reference line; and polystyrene (brown dash line) with three reference lines at 1583, 1602, and 3027 cm^{-1}; reference lines at 2926 (black solid line) and 2853 cm^{-1} (black dash line) and at 2962 (red solid line) and 2872 cm^{-1} (red dash line) corresponds to theoretically calculated asymmetrical and symmetrical stretching vibrations of methylene and methyl groups, respectively. Note: sample order is color-coded from blue to brown. (For interpretation of the references to colour in this figure legend, the reader is referred to the web version of this article.)

1869 cm^{-1} [51]. For SMA copolymers those bands are shifted by 15 cm^{-1} to lower wavenumbers – 1773 and 1855 cm^{-1}, respectively, probably due to hydrogen-bond formation. The reasons for splitting the band centered at 1869 cm^{-1} is unknown, but it may be due to intramolecular vibrations, resonance interactions, conformational isomers, or symmetric-asymmetric coupling.

For methylene group four bending vibrations (scissoring, rocking, wagging, and twisting) are usually observed in the 1150–1470 cm^{-1} region and near 720 cm^{-1}. It is worth noting that the band at 729 cm^{-1} can be found in all spectra of all pSMAnh, but it cannot be seen in the spectrum of PS, most likely due to overlapping with the more intense band at 757 cm^{-1}.

Identification of ether groups from the IR spectra is not easy, because organic compounds frequently contain other C—O bonds, e.g., alcohols, acids. Of the two ethereal C—O—C asymmetrical and symmetrical stretching vibrations, only the former one is active in IR spectroscopy [51]. Based on comparison of spectra of PS, 2-bromosuccinic anhydride, and PRO 10235 with spectra of esters, the band at 1105 cm^{-1} was assigned to asymmetrical C—O—C stretching (Fig. S4). Additionally, the absorbance at 1729 cm^{-1} was assigned to an ester carbonyl group, which is approximately 13 cm^{-1} lower than expected. As mentioned previously, this may be due to formation of inter- and intramolecular hydrogen bonds.

The presence of the 1710 cm^{-1} band in IR spectra of all Xiran® polymers may suggest that the pSMAnh are partially hydrolyzed or contain another type of carbonyl group beside the anhydride one (Fig. 3a). Moreover, the spectrum of Xiran® 40005 looks similar to the spectra of SMA® esters: the band around 1733 cm^{-1} can be assigned to an ester carbonyl group, while the ester C—O bond at 1105 cm^{-1} is present as well, but overlaps with the more intense band at 1078 cm^{-1}. To further confirm partial hydrolysis of Xiran® polymers we looked for bands corresponding to hydroxyl groups. A broad band with shoulders is present in the region of 3100–3600 cm^{-1} in the Xiran® 40005 and SMA® monoesters (1440, 17352, and 2625) spectra, which can be due to hydroxyl groups that are hydrogen-bonded to various degrees. It should be kept in mind, that the νO—H band also appears with moist samples, or samples containing water of crystallization, or alcohol. Presence of the hydroxyl group cannot be ascertained without additional analysis, especially for Xiran® 40005: its spectrum has a weak band at 1625 cm^{-1} which is characteristic for H—O—H bending

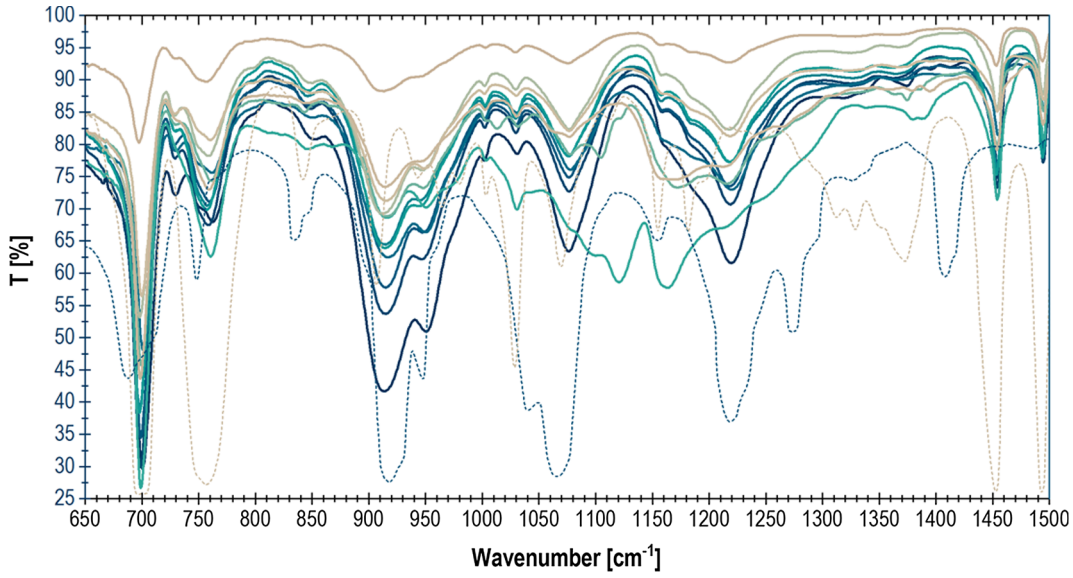

Fig. 4. IR spectra (650–1500 cm^{-1} region) of poly(styrene-co-maleic anhydrides) (solid lines) and reference substances (dash line): 1000, 30010, 2000, 40005, 3000, 25010, 1440, 17352, 2021, PRO 10235, 2625, 245 NR; 2-bromosuccinic anhydride (blue dash line) and polystyrene (brown dash line). Note: sample order is color-coded from blue to brown. (For interpretation of the references to colour in this figure legend, the reader is referred to the web version of this article.)

vibrations and can be due to the presence of water in the sample. Besides that, the spectra of 5 aforementioned ester copolymers have a band at 1171 cm^{-1} (present in succinic acid as well) attributed to C—O stretching vibrations.

Given that we have not found any characteristic bands corresponding to hydroxyl groups in spectra of Xiran® 25010 and Xiran® 30010, we may assume that those polymers are not subjected to hydrolysis but probably contain another type of carbonyl group, e.g., aldehyde group. The presence of aldehyde groups is an undesirable feature of polymers used for membrane solubilization due to possible reactions between aldehyde groups and amino groups of proteins which can cause aggregation and alter the protein structure and function.

FTIR spectroscopy was also used to verify the completion of hydrolysis of the maleic anhydride moiety. In Fig. 5, the parent SMA copolymers have distinct anhydride bands around 1770–1780 cm^{-1}. For the hydrolyzed SMA copolymers, these bands are almost completely displaced by the stretching vibrations of carboxylate ion at 1400 and 1560 cm^{-1} along with the appearance of the OH band near 3200 cm^{-1}. Presence of a band centered at 1770–1780 cm^{-1} in spectra of hydrolyzed polymers suggests that the hydrolyzed form of SMA copolymer contains a small amount (less than 5%) of anhydride groups (Fig. 5, red arrows). The degree of anhydride hydrolyses was quantified by a decrease in the integrated area of the anhydride carbonyl band from absorbance spectra after its baseline correction and normalization using internal reference bands (699 cm^{-1} for styrene).

Theoretically, FTIR spectra can be further quantified to estimate s/m ratio of SMA copolymers (Fig. S5), however, the construction of a calibration curve will be required. Though, complications due to the selection of standards and solvent may compromise this approach.

3.3. Effect of pSMA-S formulation on membrane protein extraction from spinach thylakoids

The main focus of the study was to characterize the solubilization

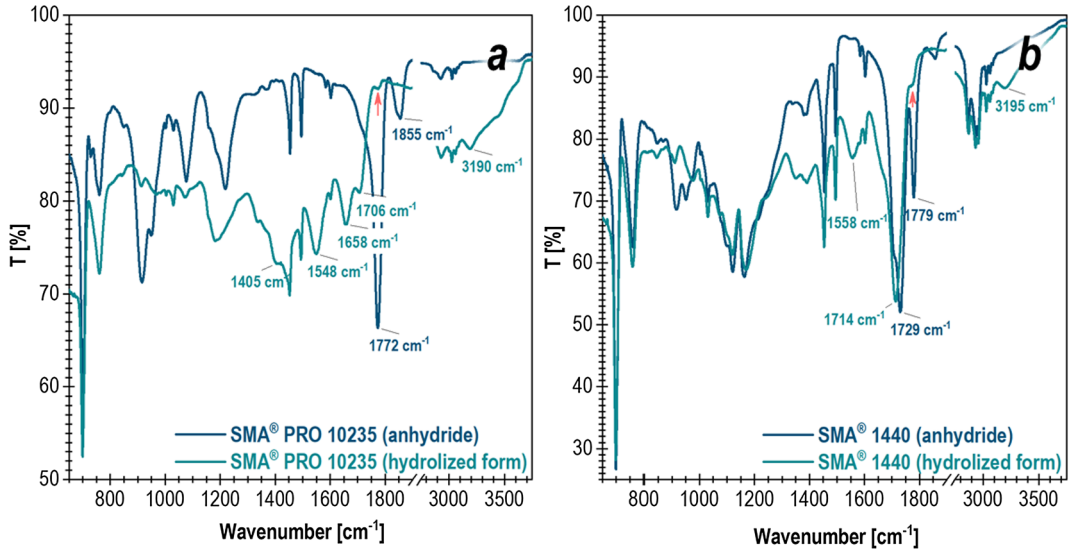

Fig. 5. IR spectra of anhydride and hydrolyzed form of SMA® PRO 10235 (*a*) and SMA® 1440 (*b*). (For interpretation of the references to colour in this figure legend, the reader is referred to the web version of this article.)

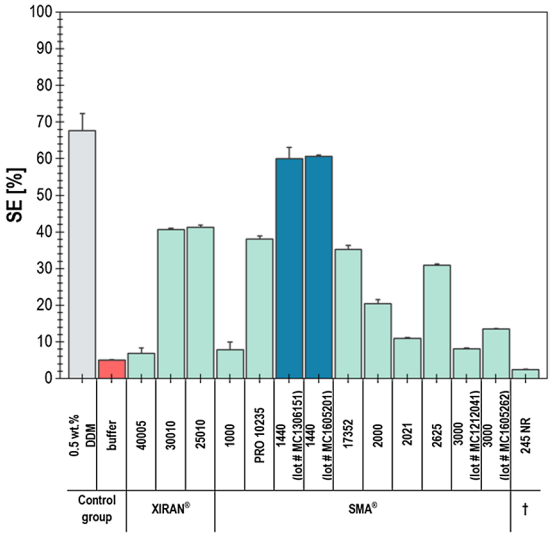

Fig. 6. Solubilization efficacy of pSMA-S (2.5 wt%) in extraction of membrane proteins from spinach thylakoid membranes based on total protein content. The solubilization was carried out for two hours at 40 °C in GKRB-150. Note: † denotes Lustran®.

efficacy of hydrolyzed copolymers as a function of their physicochemical properties. All polymers employed for solubilization trials were in their hydrolyzed ammonium or sodium salt form. Given that buffers with 150 mM KCl were able to remove peripherally associated protein complexes from crude thylakoids, the primary comparison of solubilized efficacy of SMA copolymers was carried out on washed TMs. As one can see in Fig. 6, solubilization efficacy of pSMA-S depends on the type of the polymer. The relative solubilization efficacy (based on total protein content) of the polymers decreases along the series with the top-5 SMA copolymers highlighted in bold:

SMA® 1440 > XIRAN® 25010 ≈ XIRAN® 30010 ≈ SMA® PRO 10235 ≈ SMA® 17352 > SMA® 2625 > SMA® 2000 > SMA® 3000 ≈ SMA® 2021 > Xiran® 40005 ≈ SMA® 1000 > Lustran® 245 NR.

Comparing physicochemical properties of pSMA-S we can look further into the differences in solubilizing efficacy of SMA copolymers. For example, SMA® 2021 with larger molecular weight (21.0 kDa) compared to its analog SMA® 2000 (7.5 kDa) with styrene-to-maleic ratio 2:1 solubilizes spinach thylakoid membranes but at a significantly lower efficacy ($p = 0.00473$ when equal variance is assumed): 10.9 ± 0.3 vs. 20.4 ± 1.2%. At the same time, much larger Lustran® 245 NR with 120 kDa molecular weight was not effective in extraction of membrane proteins compared to other 3:1 pSMA-S: XIRAN® 25010 (9.2 kDa) and SMA® 3000 (9.5 kDa). Even though the trend of the molecular weight effect is consistent with the previously reported observations [17,19], care should be taken in grouping polymers based on their s/m ratio or molecular weight and comparing grouped polymers, especially from different companies. As we will see further, other factors besides size and s/m ratio may affect the solubilization of biomembranes. For example, let's compare solubilization efficacy of 3:1 polymers: XIRAN® 25010 and SMA® 3000. Even though there is an approximately 5% difference between the two lots of SMA® 3000 which can be explained by batch-to-batch variability, there is almost a four-fold increase of SE when SMA® 3000 is substituted with XIRAN® 25010. Given that there is no straightforward correlation between solubilization efficacy of pSMA-S and their physical properties (Fig. S6, Table S V, and [17,19]), one can assume that polymer chemistry and interfacial phenomena plays a crucial role in lipid solubilization and membrane protein extraction. Distribution of monomer units along the polymer chain and polymer tacticity are expected to affect their solubilization efficacy as well.

It has been reported in previous studies that polymers with styrene-to-maleic ratio 2:1 and 3:1 are the most efficient in lipid and membrane protein solubilization, while polymers with other molar ratios are less effective or not effective at all [17,19]. But as one can see in Fig. 6, SMA® PRO 10235 with s/m ratio 1.5 has the same solubilization efficacy (within the error) as 3: 1 XIRAN® 25010 and 2:1 XIRAN® 30010: 38.1 ± 0.9 compared to 41.3 ± 0.6 and 40.7 ± 0.3, respectively. *The fact that pSMA-S with a s/m ratio less than 2 still can be as efficient in membrane protein extraction as 2:1 and 3:1 polymers is novel and emphasizes the importance of chemical properties of SMA copolymers over physical polymer characteristics.* Thus, adjusting chemical properties of SMA copolymers either during the polymer synthesis or after it via post-polymerization modifications creates the possibility to improve lipid solubilization and extraction of membrane proteins. For example, partial esterification of SMA® PRO 10235 with butoxyethanol (SMA® 1440) increases SE, while introduction of cyclohexyl and isopropyl ester groups (SMA® 17352) causes a decrease in membrane protein extraction (Figs. 6 and 7). For partial propyl monoester SMA® 2625 direct

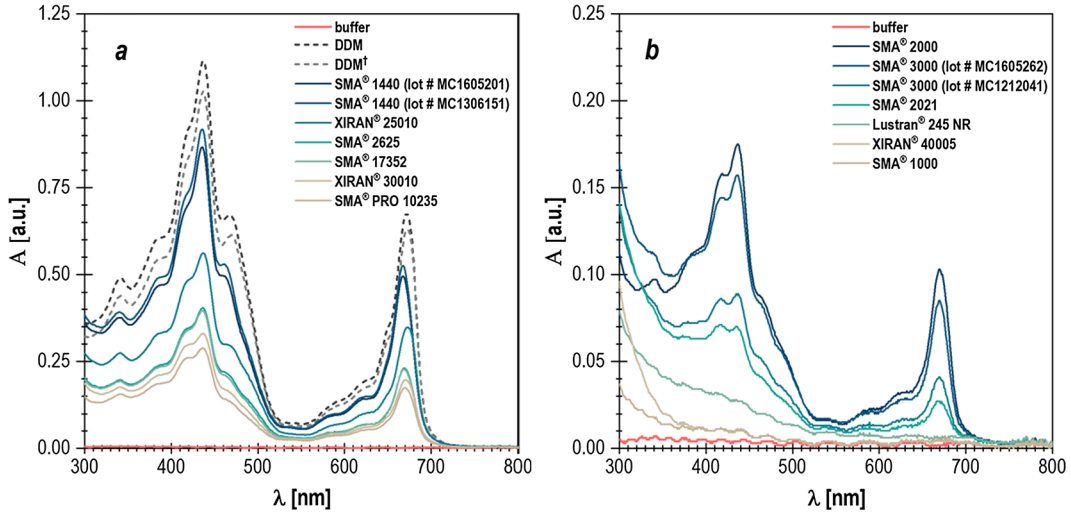

Fig. 7. UV–visible spectra of solubilized complexes in GKRB-150 at pH 8.50. The final concentration of DDM and pSMA-S was 0.5 and 2.5 wt%, respectively. The solubilization was carried out for two hours at 40 °C in GKRB-150. Note: † stands for 20 °C. (For interpretation of the references to colour in this figure legend, the reader is referred to the web version of this article.)

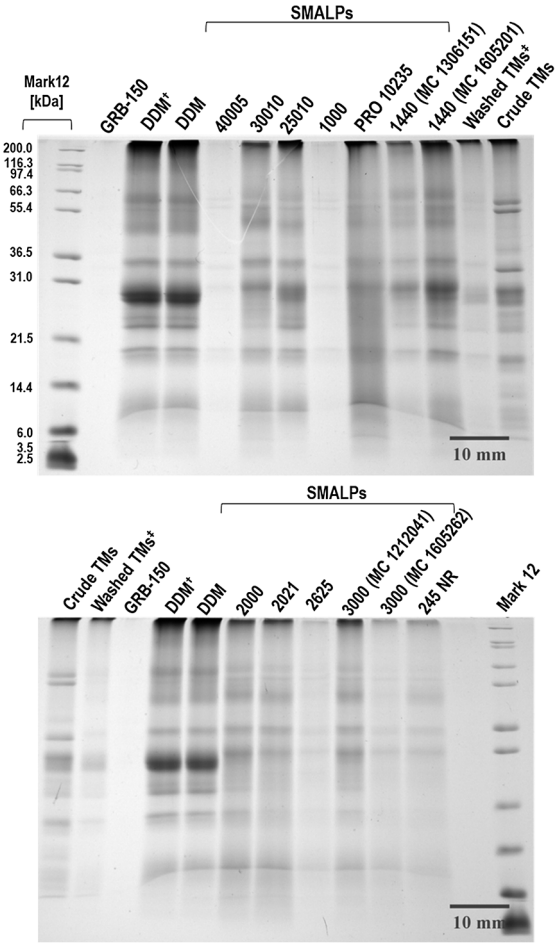

Fig. 8. Coomassie staining of thylakoid membrane proteins separated on 15% glycine-SDS-PAGE. The final concentration of DDM and pSMA-S was 0.5 and 2.5 wt%, respectively. The solubilization was carried out for two hours at 40 °C in GKRB-150. Note: † stands for 20 °C, ‡ stands for TMs washed with 100 mM Na_2CO_3.

comparison is not possible given that we did not have a matching or similar polymer or its precursor. But despite that fact, SMA® 2625 solubilizes 31.0 ± 0.3% of spinach membrane proteins and its solubilization efficacy is significantly higher ($p = 0.00014$ when equal variance is assumed) in comparison to the rest of SMA copolymers (excluding the top-5), for which the average SE is 10.1 ± 2.4%.

Solubilization efficacy determined by different methods based either on estimation of protein or pigment concentration have a similar trend (Table S VI), even though the order of polymers differ slightly. These variations in polymer series can suggest differential affinity of SMA copolymers towards lipids, proteins and/or pigments such as chlorophylls and carotenoids, and have to be addressed in further studies.

The polypeptide profile of protein-containing SMALPs was analyzed by SDS-PAGE. As one can see in Fig. 8, the polypeptide profile of membrane protein complexes extracted by DDM (0.5 wt%) and SMA copolymers (2.5 wt%) are very similar to the polypeptide profile of TMs, even though a slight variation in band relative intensities is observed between different extracted protein complexes.

Besides proteins, SMA copolymers also get separated by electrophoresis and stained with CBB R-250. Their interference with SDS-PAGE is tolerable up to polymer concentration in the sample approximately 3 wt%, but in general SMA copolymers with the concentration higher than 5 wt% or with high molecular weights (e.g., 120 kDa) cause significant smearing of protein bands (data not shown here). This is presumably due to co-migration of the negatively charged SMA copolymers with a mobility similar to some of the lower molecular weight proteins.

To improve the electrophoretic separation and subsequent CBB staining we were able to selectively precipitate the proteins in 25% TCA (see Section 2.12 for details) away from the SMA copolymers and other interfering substances followed by centrifugation and washing with cold acetone (data not shown). This method successfully removes SMA copolymers from samples except of SMA® PRO 10235, for reasons at this point in time we cannot explain.

Based on relative intensities of protein bands one can see a good agreement between SDS-PAGE results and determined total protein content. It is also clear that there are specific protein subunits that appear to be extracted preferentially by most of the SMA copolymers. Further proteomic analysis by tandem mass spectroscopy will help to precisely identify and quantify the membrane proteins extracted with different types of SMA copolymers after SMALPs separation. We have already begun separating SMALPs utilizing isopycnic centrifugation (density-based technique) and native electrophoresis (based on size and charge; see Section 3.5).

3.4. Effect of external factors on membrane protein extraction from spinach thylakoids

From previous studies it is known that beside SMA copolymer formulation, external factors such as pH, presence of divalent cations, organization of lipid bilayer, and lipid-to-protein ratio effect the solubilization efficacy of pSMA-S. To overcome these complications and increase the yield of protein-containing SMALPs, a few strategies can be used, namely:

1. Solubilization of lipids and extraction of membrane protein complexes from biomembranes at pH higher than approximately 8;
2. Removal of divalent cations in sample by extensive successive prewashing or washing of lipid membranes and biomembranes with chelating agents, for example, ethylenediaminetetraacetic acid (EDTA) salts;
3. Application of solutions with increased ionic strength during lipid solubilization and membrane protein extraction for screening the repulsive forces between negatively charged lipid membranes and polymers;
4. Increase in lipid-to-protein ratio of biomembranes by *in situ* alterations or fusion with synthetic lipids [17];
5. Solubilization of membrane and biomembranes at temperatures above lipid phase transition;
6. Removal of peripherally associated proteins from biomembranes in order to facilitate the access of pSMA-S to the integral membrane proteins of interest.

Many protocols for chloroplast [54] and thylakoid membrane [55] isolation include the addition of Mn^{2+} and Mg^{2+} ions to buffers. Application of buffers with these divalent cations can be explained by a few reasons. For many years it has been known that oxygen-evolving photosynthetic organisms require manganese for their normal growth [56]. It has also been observed that addition of Mn^{2+} ions helps to maintain the Mn_4CaO_5 cluster associated with the oxygen evolving complex in photosystem II (PSII) and increases its oxygen evolving activity [56,57]. From other side, the most striking feature of thylakoid membrane structure, controlled by cation concentration, is stacking of these membranes, as it is in grana of intact chloroplasts. The role of magnesium in thylakoid structure has been observed from early work [58] which indicated that ultrastructure of thylakoid membranes is sensitive to the presence/absence of Mg^{2+} cations. It has also been observed by multiple methods *in vitro* that stacked thylakoid membranes separate or unstack when placed into low-ionic-strength buffers [59,60]. In contrast, upon the addition of appropriate concentrations of

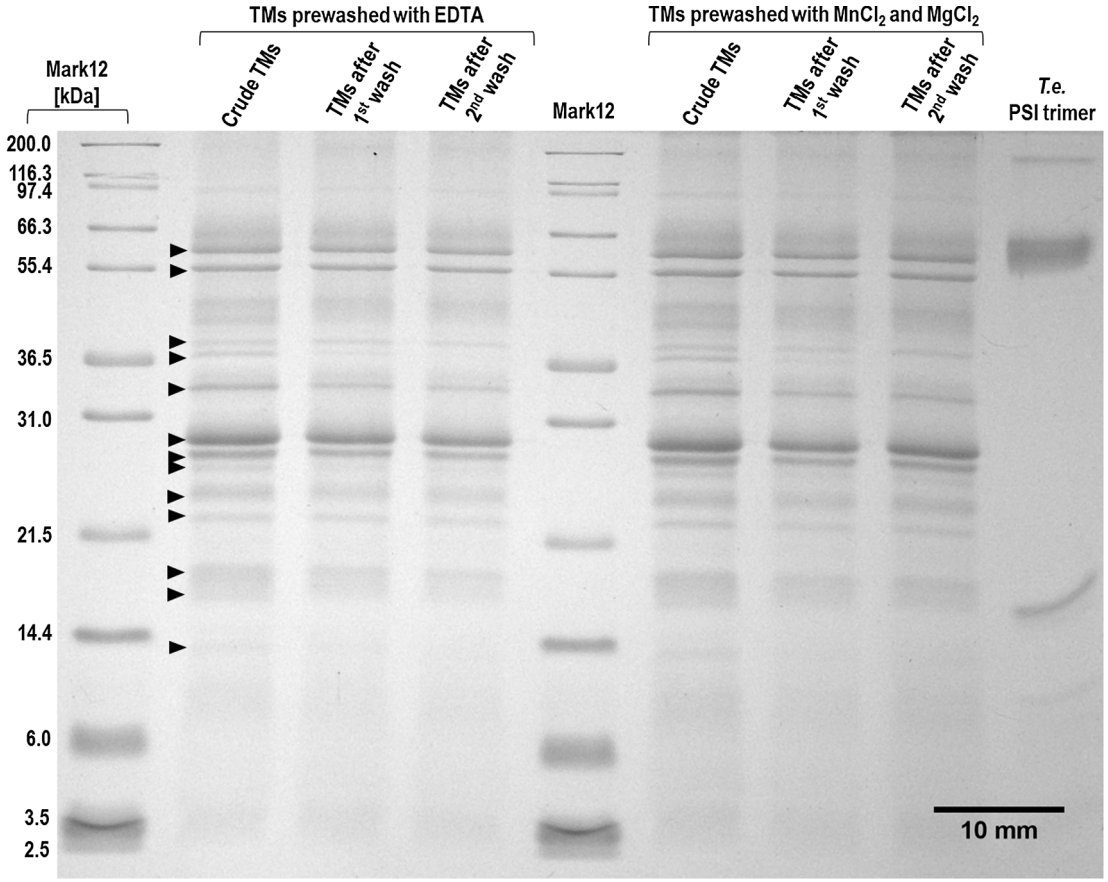

Fig. 9. Coomassie staining of proteins form crude thylakoid membranes and thylakoid membranes after 1st and 2nd wash with GKB-150 separated on 15% glycine-SDS-PAGE. Note: lane 9 represents *Thermosynechococcus elongatus* BP-1 PSI trimer (as a control).

monovalent or divalent cations, especially Mg^{2+}, these membranes undergo spontaneous grana formation. This has been postulated to be due to enhanced electrostatic screening of negative charges associated with the phosphorylation of the light-harvesting chlorophyll *a/b* protein (LHCP) complexes located within the thylakoid membranes. In light of these observations, we have explored how SMA copolymers interact with thylakoids that are replete with these two cations vs. those that are depleted by extensive successive prewashing or EDTA pretreatment.

Prewashing crude TMs with 3 mM Mn^{2+} and 3 mM Mg^{2+} is supposed to maintain the oxygen evolving activity and keep the thylakoids stacked, while prewashing the crude TMs with 5 mM EDTA salt is expected to remove free divalent cations and cause unstacking of grana. Even though there is no obvious difference in polypeptide profile of TMs prewashed with EDTA or divalent cations (Fig. 9), according to our preliminary data, prewashing step with EDTA sodium salt allow increasing the solubilization efficacy (based on absorbance) for all SMA copolymers. For example, efficacy of XIRAN® 25010 to solubilize EDTA prewashed TMs is on average seven times higher compared to Me prewashed biomembranes, even though no polymer concentration dependency (Fig. S7) on solubilization efficacy was observed. A similar effect can also be achieved by extensive successive prewashing which removes free divalent cations.

During solubilization trials with crude TMs we also found out that peripherally associated protein complexes can be removed from thylakoids by buffers containing 150 mM KCl. As one can see in Fig. 9 polypeptide profile of crude TMs consists of at least 22 bands. The band molecular weights showed in arrowheads were estimates to be 60.2, 55.4, 39.9, 38.3, 33.9, 28.7, 27.7, 26.6, 24.5, 22.9, 18.9, 17.2, and approximately 13 kDa. Washing TMs with GKB-150 almost completely remove proteins with molecular weight 38.3 and 26.6 kDa. The polypeptide profile of stromal and peripherally associated proteins can be found in SI (Figs. S8 and S9).

Removal of stromal and peripherally associated proteins from thylakoids with 100 mM sodium carbonate or chaotropic agent (1 M NaBr) improves significantly extraction of membrane protein complexes for all SMA copolymers by decreasing non-specific protein solubilization due to increased ionic strength without affecting the polypeptide profile of extracted protein-containing SMALPs (data not shown).

Based on our preliminary data, sodium carbonate treatment is more effective in removing of stromal and peripherally associated proteins compared to treatment with GKB-150 or GKB-150 containing 1 M NaBr (Fig. 10, Fig. S9). According to Fujiki et al. [31], the effectiveness of carbonate treatment is determined primarily by pH of the solutions rather than solution ionic strength.

Even though we showed that removal of stromal and peripherally associated protein complexes from biomembranes facilitate the access of pSMA-S to the integral membrane proteins, more detail and systematic study is required to understand the fundamentals of membrane protein solubilization by SMA copolymers and effect of different pretreatment conditions on structural and functional properties of membrane protein complexes.

3.5. Characterization of protein-containing SMALPs

Fluorescence of soluble fractions containing SMALPs depends on type of copolymer used for solubilization of thylakoid membranes and on membrane prewashing step (Fig. 11). Prewashing crude TMs with 5 mM EDTA sodium salt increases the fluorescence and, as it was shown previously, solubilization efficacy (based on chlorophyll) of SMA copolymers.

Fractionation of spinach thylakoid membranes into PSI- and PSII-

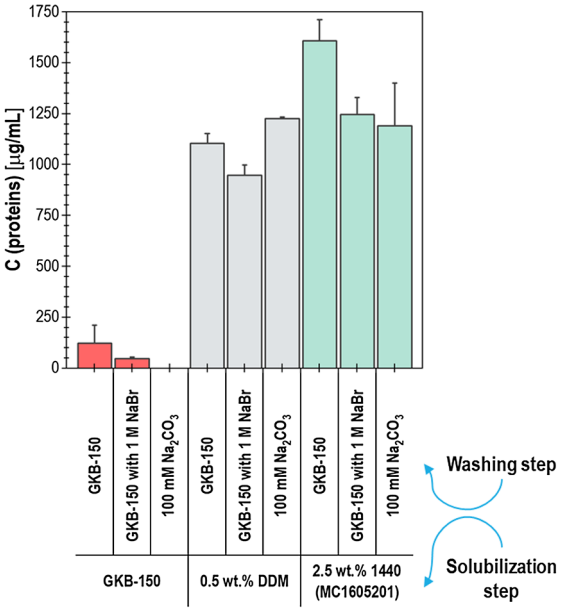

Fig. 10. Protein concentration of protein complexes extracted from thylakoid membranes previously washed with GKB-150 (pH 8.64), GKB-150 with 1 M NaBr (pH 8.79), and with 100 mM Na_2CO_3 (pH 10.88). Membrane proteins were solubilized using GKB-150 (negative control), 0.5 wt% DDM (positive control), and 2.5% 1440 (MC 1605201).

enriched fractions confirmed the assignments of chlorophyll fluorescence emission bands within 685–695 nm region to PSII complex and the emission band at 720 nm to PSI complex. In general, chlorophyll low temperature fluorescence emission spectra of spinach thylakoid membranes consist of a few main components emitting at 680 nm (LHCII), 685 nm (CP47/CP43), 695 nm (CP47), 700 nm (aggregated LHCII trimer), 720 nm (PSI core complex), and 735 nm (LHCI) [61]. Even though we have not found statistically significant difference in chlorophyll *a*/*b* ratio based on its extraction with 80 vol% aqueous acetone solutions (Fig. S10), which is on average is 3.1 ± 0.8, the LT fluorescence data shows the presence of at least two different chlorophyll-containing complexes. The LT fluorescence emission profile and 680-to-720 nm ratio (based on area) (Fig. 11d) differ between SMA formulations and will be further studied in more details for each protein-containing SMALP fraction separately.

For separation of native SMALPs we utilized an electrophoretic technique, namely, CN-PAGE. Among the five different buffer formulations we tested, GB-0 provides the best resolution of SMALPs for reasons that remain unknown. In general, the number of bands and the electrophoretic mobility of SMALPs vary among different formulation of SMA copolymers. Some SMALPs, for example, based on XIRAN® 25010 aggregate upon loading into the well complicating their electrophoretic separation and purification. As it is shown in Fig. 12, it would appear that the SMA® 1440 solubilizes at least 4 distinct complexes with different sizes and net charges. The number of bands and electrophoretic mobility of SMALPs differ from the ones for DDM solubilized sample. SMALPs with a net negative charge due to deprotonated carboxyl groups have higher electrophoretic mobilities compared

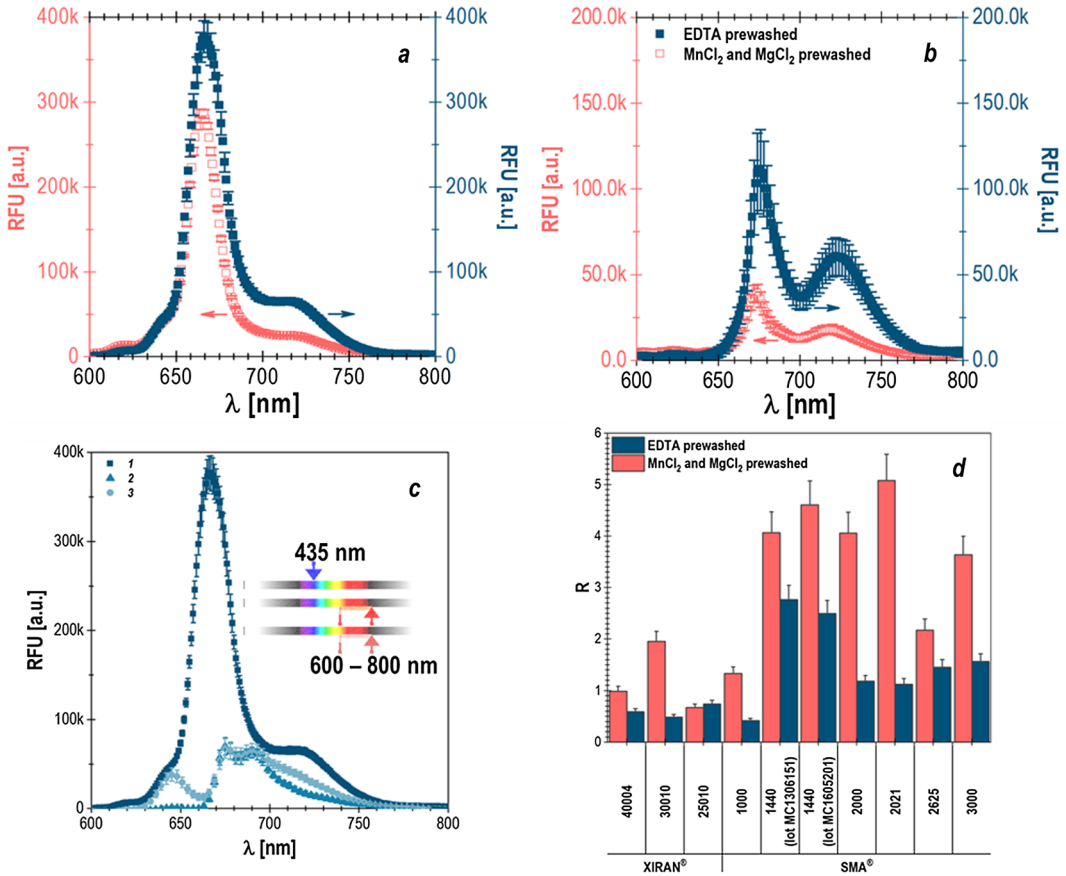

Fig. 11. Low temperature fluorescence emission spectra of unpurified SMALPs: *a* – soluble fraction after treatment of prewashed crude thylakoid membranes with 2.5 wt% SMA® 1440; *b* – soluble fraction after treatment of prewashed crude thylakoid membranes with 2.5 wt% XIRAN® 25010; *c* – soluble (1), insoluble (2) fractions and sample before centrifugation (3) after treatment of EDTA prewashed crude thylakoid membrane with 2.5 wt% SMA® 1440; *d* – area ratio (R) of peaks at 680 and 720 nm after the deconvolution of the emission spectra. The spectra were measured upon excitation at 435 nm in 600–800 nm wavelength range (see insert to *c*). (For interpretation of the references to colour in this figure legend, the reader is referred to the web version of this article.)

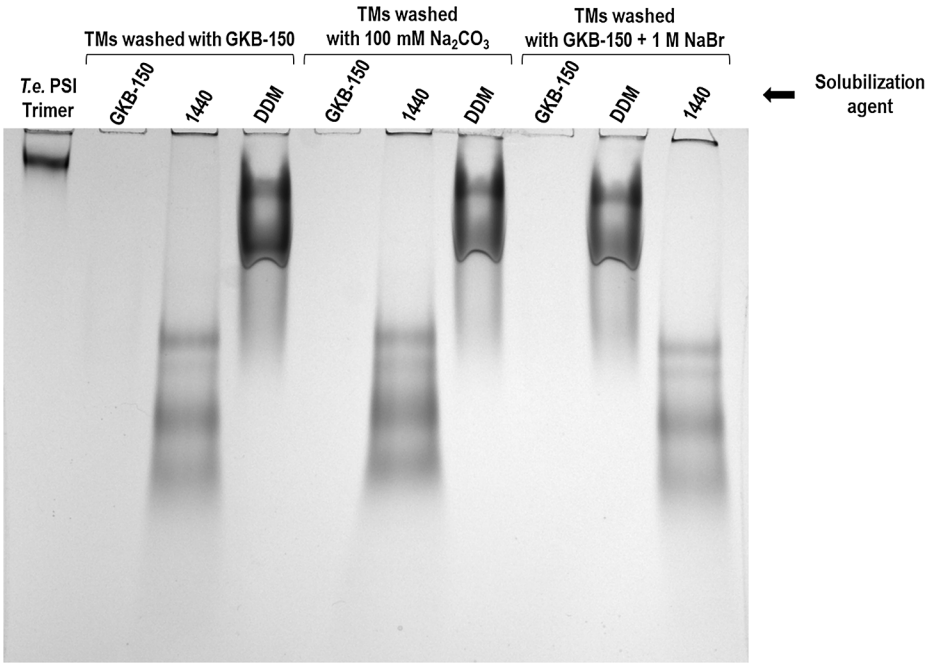

Fig. 12. Coomassie staining of membrane proteins extracted by SMA® 1440 (2.5 wt%) and DDM (0.5 wt%) and separated using 3–9% step gradient CN-PAGE.

to biomembranes solubilized by neutral DDM. Overall, results obtained from CN-PAGE and isopycnic centrifugation using sucrose gradients (data not shown here) agree well with each other.

As it is known thylakoid membranes contain four major complexes associated with photosynthetic light harvesting, electron transport, and ATP synthesis. These major complexes include photosystems I and II, trimeric light-harvesting complex (LHCII), the cytochrome b_6/f complex (b_6/f), and the proton ATPase (CF_0/CF_1). To find out which of these complexes, if any, were extracted by SMA® 1440, we have investigated the presence or absence of these complexes by performing immunoblot analysis of an unpurified SMALP fraction (based on 1440 polymer), that was separated using 15% tricine-SDS-PAGE. In our preliminary study, we tested 9 different antibodies against one or more subunits from these various complexes. Immunoblot results suggest that the protein-containing SMALPs (based on 1440 polymer) contain varying amounts of PSII, LHCII, and PSI. This was clear from the cross-reactivity against PsbA, CAB/LHCII, and PsaC, respectively (Fig S11). Further, we saw no evidence that the SMALPs contain CF_0/CF_1 ATPase (no cross-reactivity against the α- and γ-subunit of CF_1). Although there is some cross-reactivity with the cyt b_6 antibody, the molecular weight is too high to be b_6/f complex, plus the lack of cross-reactivity to subunit IV suggests that the SMA treatment of the crude thylakoids does not release the b_6/f complex. Although it may be possible that these subunits are presented at levels below detection limits. It is also apparent that SMA treatment did not release any of the RuBisCo holoenzyme since the immunoblot analysis did not detect any cross-reactivity to the L-subunit of RuBisCo. This may suggest that the procedure for isolation of thylakoid membranes was effective in removing this highly abundant and often cross-reactive complex. However, it is clear that the treatment does release PSII, LHCII and PSI. The organization of these three complexes is not yet known and the fact that we observe by CN-PAGE at least four complexes with different sizes suggests that there are multiple supramolecular protein complexes. Future work will address the identity and composition of these distinct complexes by a combination of native electrophoresis, proteomics via tandem mass spectroscopy, and single-particle cryo-TEM analysis.

4. Conclusions

SMA copolymers can extract membrane proteins from spinach thylakoid membranes with different degrees of efficacy. Of the twelve commercially available copolymers studied, SMA® 1440 ranked first in solubilizing thylakoid membranes followed by XIRAN® 25010, XIRAN® 30010, SMA® PRO 10235, and SMA® 17352. It remains inconclusive which SMA copolymer properties are attributed to high membrane protein extraction from thylakoid membranes. The butoxyethanol group on SMA® 1440, resulting from esterification of SMA® PRO 10235, may be a key to more successful protein extraction for reasons that remain unknown.

5. Authors' declaration

Authors warrant that the article is their original work, has not received prior publication, and is not under consideration for publication elsewhere. If accepted, the work will not be published elsewhere in the same form, in English or in any other language, including electronically without the written consent of the copyright holder. All authors have seen and approved the version of the manuscript being submitted.

6. Authors' contributions

OK and BB supervised this work, helped in the analysis and interpretation of data, and, together with JM, KGA, and JH worked on writing and revising the manuscript. OK and JH carried out isolation of chloroplasts from *Spinacia oleracea,* preparation and isolation of thylakoid membranes, and performed immunoblot analysis. OK and KGA characterized polymers using FTIR, while OK and JM performed all other experiments. Data processing and visual representation was done by OK together with JM.

Funding

Support to B.D.B. and O.K. has been provided from the Gibson

Family Foundation, the UTK/ORNL Science Alliance, the Tennessee Plant Research Center, a JDRD Award to B.D.B., the Dr. Donald L. Akers Faculty Enrichment Fellowship to B.D.B.

Conflict of interest

The authors declare that there's no financial or personal interest or believes that could affect their objectivity.

Acknowledgments

Authors thanks **Victor Marik** and **Nathan Brady** for proofreading the paper and discussing the results, and **Alexander Strizhak** and **Tony Ladd** for helpful comments. Authors thank **Ryan Beer** and **Bill Dougherty** from Total Cray Valley for consulting, technical assistance, and greatly appreciate **Total Cray Valley** support of the research by providing samples of SMA copolymers. Also, authors thanks **Pieter Hanssen** from Polyscope Polymers B.V. for technical assistance, and Polyscope Polymers B.V. for providing SMA polymers samples; **Jeffrey Rickle** from **INEOS Styrolution America LLC** for providing a sample of high molecular SMA polymer; and **Cherie Stabler** for sharing Frontier FT-IR spectrometer (Perkin Elmer).

Data availability

The raw/processed data required to reproduce these findings are available upon request.

Appendix A. Supplementary material

Supplementary data to this article can be found online at https://doi.org/10.1016/j.eurpolymj.2018.10.035.

References

[1] T. Ravula, N.Z. Hardin, S.K. Ramadugu, S.J. Cox, A. Ramamoorthy, Formation of pH-resistant monodispersed polymer–lipid nanodiscs, Angew. Chemie - Int. Ed. 57 (2018) 1342–1345, https://doi.org/10.1002/anie.201712017.
[2] L.I. Osipow, Surface Chemistry: Theory and Industrial Applications, Reinhold Publishing Corporation, New York, 1962.
[3] S.R. Tonge, B.J. Tighe, Responsive hydrophobically associating polymers: a review of structure and properties, Adv. Drug Deliv. Rev. 53 (2001) 109–122, https://doi.org/10.1016/S0169-409X(01)00223-X.
[4] S.R. Tonge, B.J. Tighe, Lipid-containing compositions and uses thereof, US6436905B1, 2002.
[5] S. Tonge, Compositions comprising a lipid and copolymer of styrene and maleic acid, PCT/GB2006/050134, 2006.
[6] S. Scheidelaar, M.C. Koorengevel, J.D. Pardo, J.D. Meeldijk, E. Breukink, J.A. Killian, Molecular model for the solubilization of membranes into nanodisks by styrene maleic acid copolymers, Biophys. J. 108 (2015) 279–290, https://doi.org/10.1016/j.bpj.2014.11.3464.
[7] J.J. Dominguez Pardo, J.M. Dörr, A. Iyer, R.C. Cox, S. Scheidelaar, M.C. Koorengevel, V. Subramaniam, J.A. Killian, Solubilization of lipids and lipid phases by the styrene–maleic acid copolymer, Eur. Biophys. J. 46 (2017) 91–101, https://doi.org/10.1007/s00249-016-1181-7.
[8] S.C. Lee, T.J. Knowles, V.L.G. Postis, M. Jamshad, R.A. Parslow, Y. Lin, A. Goldman, P. Sridhar, M. Overduin, S.P. Muench, T.R. Dafforn, A method for detergent-free isolation of membrane proteins in their local lipid environment, Nat. Protoc. 11 (2016) 1149–1162, https://doi.org/10.1038/nprot.2016.070.
[9] A.J. Bell, L.K. Frankel, T.M. Bricker, High yield non-detergent isolation of photosystem I-light-harvesting chlorophyll II membranes from spinach thylakoids: Implications for the organization of the PS I antennae in higher plants, J. Biol. Chem. 290 (2015) 18429–18437, https://doi.org/10.1074/jbc.M115.663872.
[10] J.M. Dörr, M.H. van Coevorden-Hameete, C.C. Hoogenraad, J.A. Killian, Solubilization of human cells by the styrene–maleic acid copolymer: insights from fluorescence microscopy, Biochim. Biophys. Acta - Biomembr. 2017 (1859) 2155–2160, https://doi.org/10.1016/j.bbamem.2017.08.010.
[11] N. Voskoboynikova, W. Mosslehy, A. Colbasevici, T.T. Ismagulova, D.V. Bagrov, A.A. Akovantseva, P.S. Timashev, A.Y. Mulkidjanian, V.N. Bagratashvili, K.V. Shaitan, M.P. Kirpichnikov, H.-J. Steinhoff, Characterization of an archaeal photoreceptor/transducer complex from Natronomonas pharaonis assembled within styrene–maleic acid lipid particles, RSC Adv. 7 (2017) 51324–51334, https://doi.org/10.1039/C7RA10756K.
[12] S.C. Lee, N.L. Pollock, Membrane proteins: is the future disc shaped? Biochem. Soc. Trans. 44 (2016) 1011–1018, https://doi.org/10.1042/BST20160015.
[13] M. Jamshad, Y. Lin, T.J. Knowles, R.A. Parslow, C. Harris, M. Wheatley, D.R. Poyner, R.M. Bill, O.R.T. Thomas, M. Overduin, T.R. Dafforn, Surfactant-free purification of membrane proteins with intact native membrane environment, Biochem. Soc. Trans. 39 (2011) 813–818, https://doi.org/10.1042/BST0390813.
[14] V. Schmidt, J.N. Sturgis, Modifying styrene-maleic acid co-polymer for studying lipid nanodiscs, Biochim. Biophys. Acta - Biomembr. 2018 (1860) 777–783, https://doi.org/10.1016/j.bbamem.2017.12.012.
[15] J.M. Dörr, S. Scheidelaar, M.C. Koorengevel, J.J. Dominguez, M. Schäfer, C.A. van Walree, J.A. Killian, The styrene–maleic acid copolymer: a versatile tool in membrane research, Eur. Biophys. J. 45 (2016) 3–21, https://doi.org/10.1007/s00249-015-1093-y.
[16] M. Esmaili, M. Overduin, Membrane biology visualized in nanometer-sized discs formed by styrene maleic acid polymers, Biochim. Biophys. Acta - Biomembr. 2018 (1860) 257–263, https://doi.org/10.1016/j.bbamem.2017.10.019.
[17] D.J.K. Swainsbury, S. Scheidelaar, N. Foster, R. van Grondelle, J.A. Killian, M.R. Jones, The effectiveness of styrene-maleic acid (SMA) copolymers for solubilisation of integral membrane proteins from SMA-accessible and SMA-resistant membranes, Biochim. Biophys. Acta - Biomembr. 2017 (1859) 2133–2143, https://doi.org/10.1016/j.bbamem.2017.07.011.
[18] J.J. Dominguez Pardo, J.M. Dörr, A. Iyer, R.C. Cox, S. Scheidelaar, M.C. Koorengevel, V. Subramaniam, J.A. Killian, SI: Solubilization of lipids and lipid phases by the styrene–maleic acid copolymer, Eur. Biophys. J. 46 (2017).
[19] K.A. Morrison, A. Akram, A. Mathews, Z.A. Khan, J.H. Patel, C. Zhou, D.J. Hardy, C. Moore-Kelly, R. Patel, V. Odiba, T.J. Knowles, M.-H. Javed, N.P. Chmel, T.R. Dafforn, A.J. Rothnie, Membrane protein extraction and purification using styrene-maleic acid (SMA) copolymer: effect of variations in polymer structure, Biochem. J. 473 (2016) 4349–4360, https://doi.org/10.1042/BCJ20160723.
[20] M. Jamshad, V. Grimard, I. Idini, T.J. Knowles, M.R. Dowle, N. Schofield, P. Sridhar, Y. Lin, R. Finka, M. Wheatley, O.R.T. Thomas, R.E. Palmer, M. Overduin, C. Govaerts, J.-M. Ruysschaert, K.J. Edler, T.R. Dafforn, Structural analysis of a nanoparticle containing a lipid bilayer used for detergent-free extraction of membrane proteins, Nano Res. 8 (2015) 774–789, https://doi.org/10.1007/s12274-014-0560-6.
[21] N.G. Brady, M. Li, Y. Ma, B.D. Bruce, Non-detergent isolation of a cyanobacterial photosystem I using styrene-maleic acid alternating copolymers, Press. (n.d.).
[22] S. Rajesh, T. Knowles, M. Overduin, Production of membrane proteins without cells or detergents, N. Biotechnol. 28 (2011) 250–254, https://doi.org/10.1016/j.nbt.2010.07.011.
[23] E. Sauvage, D.A. Amos, B. Antalek, K.M. Schroeder, J.S. Tan, N. Plucktaveesak, R.H. Colby, Amphiphilic maleic acid-containing alternating copolymers - 1. Dissociation behavior and compositions, J. Polym. Sci. Part B Polym. Phys. 42 (2004) 3571–3583, https://doi.org/10.1002/polb.20202.
[24] N.L. Pollock, S.C. Lee, J.H. Patel, A.A. Gulamhussein, A.J. Rothnie, Structure and function of membrane proteins encapsulated in a polymer-bound lipid bilayer, Biochim. Biophys. Acta - Biomembr. 2017 (1860) 809–817, https://doi.org/10.1016/j.bbamem.2017.08.012.
[25] A.O. Oluwole, B. Danielczak, A. Meister, J.O. Babalola, C. Vargas, S. Keller, Solubilization of membrane proteins into functional lipid-bilayer nanodiscs using a diisobutylene/maleic acid copolymer, Angew. Chemie Int. Ed. 56 (2017) 1919–1924, https://doi.org/10.1002/anie.201610778.
[26] A. Mershin, K. Matsumoto, L. Kaiser, D. Yu, M. Vaughn, M.K. Nazeeruddin, B.D. Bruce, M. Graetzel, S. Zhang, Self-assembled photosystem-I biophotovoltaics on nanostructured TiO_2 and ZnO, Sci. Rep. 2 (2012) 234, https://doi.org/10.1038/srep00234.
[27] J. Ridge Carter, D.R. Baker, T. Austin Witt, B.D. Bruce, Enhanced photocurrent from photosystem I upon in vitro truncation of the antennae chlorophyll, Photosynth. Res. 127 (2016) 161–170, https://doi.org/10.1007/s11120-015-0162-5.
[28] I.J. Iwuchukwu, M. Vaughn, N. Myers, H. O'Neill, P. Frymier, B.D. Bruce, Nanoscale photosynthesis: photocatalytic production of hydrogen by platinized photosystem I reaction centers, Nat. Nanotechnol. 5 (2010) 73–79, https://doi.org/10.1038/nnano.2009.315.
[29] J.F. Millsaps, B.D. Bruce, J.W. Lee, E. Greenbaum, Nanoscale photosynthesis: photocatalytic production of hydrogen by platinized photosystem I reaction centers, Photochem. Photobiol. 73 (2007) 630–635, https://doi.org/10.1562/0031-8655(2001) 0730630NPPPOH2.0.CO2.
[30] B.D. Bruce, S. Perry, J. Froehlich, K. Keegstra, *In vitro* import of proteins into chloroplasts, in: S.B. Gelvin, R.A. Schilperoort (Eds.), Plant Mol. Biol. Man., Springer Netherlands, Dordrecht, 1994, pp. 497–511, , https://doi.org/10.1007/978-94-011-0511-8_32.
[31] Y. Fujiki, A.L. Hubbard, S. Fowler, P.B. Lazarow, Isolation of intracellular membranes by means of sodium carbonate treatment: application to endoplasmic reticulum, J. Cell Biol. 93 (1982) 97–102 (accessed May 31, 2018), http://www.ncbi.nlm.nih.gov/pubmed/7068762.
[32] D.I. Arnon, Copper enzymes in isolated chloroplasts polyphenoloxidase in Beta vulgaris, Plant Physiol. 24 (1949) 1–15 (accessed May 31, 2018), https://www.ncbi.nlm.nih.gov/pmc/articles/PMC437905/pdf/plntphys00263-0011.pdf.
[33] R.J. Porra, W.A. Thompson, P.E. Kriedemann, Determination of accurate extinction coefficients and simultaneous equations for assaying chlorophylls a and b extracted with four different solvents: verification of the concentration of chlorophyll standards by atomic absorption spectroscopy, Biochim. Biophys. Acta - Bioenerg. 975 (1989) 384–394, https://doi.org/10.1016/S0005-2728(89)80347-0.
[34] H. Schägger, Tricine–SDS-PAGE, Nat. Protoc. 1 (2006) 16–22, https://doi.org/10.1038/nprot.2006.4.
[35] U.K. Laemmli, Cleavage of structural proteins during the assembly of the head of bacteriophage T4, Nature 227 (1970) 680–685, https://doi.org/10.1038/227680a0.

[36] T. McLean, Electrophoresis buffers for polyacrylamide gels at various pH, Anal. Biochem. 126 (1982) 94–99 (accessed June 9, 2018), https://ac.els-cdn.com/0003269782901130/1-s2.0-0003269782901130-main.pdf?_tid=70840586-ba2a-4f12-819c-0ef30cf16dcd&acdnat=1528551067_031b3631948fd67bd67ccc0999cdf09a.
[37] Succinic anhydride, bromo-, (n.d.), https://webbook.nist.gov/cgi/cbook.cgi?ID=B6006842&Units=SI&Mask=80#IR-Spec (accessed June 9, 2018).
[38] Butanedioic acid, (n.d.), https://webbook.nist.gov/cgi/cbook.cgi?ID=C110156&Units=SI&Type=IR-SPEC&Index=1#IR-SPEC (accessed June 9, 2018).
[39] C. Ferregut, S. Nazarian, K. Vennalaganti, C.-C. Chang, V. Kreinovich, Fast error estimates for indirect measurements: applications to pavement engineering, Reliab. Comput. 2 (1996) 219–228.
[40] R. CuevasArenas, J. Klingler, C. Vargas, S. Keller, Influence of lipid bilayer properties on nanodisc formation mediated by styrene/maleic acid copolymers, Nanoscale 8 (2016) 15016–15026, https://doi.org/10.1039/C6NR02089E.
[41] A. Grethen, A.O. Oluwole, B. Danielczak, C. Vargas, S. Keller, Thermodynamics of nanodisc formation mediated by styrene/maleic acid (2:1) copolymer, Sci. Rep. 7 (2017) 11517, https://doi.org/10.1038/s41598-017-11616-z.
[42] D.J.K. Swainsbury, M.S. Proctor, A. Hitchcock, M.L. Cartron, P. Qian, E.C. Martin, P.J. Jackson, J. Madsen, S.P. Armes, C.N. Hunter, Probing the local lipid environment of the *Rhodobacter sphaeroides* cytochrome *bc1* and *Synechocystis sp.* PCC 6803 cytochrome *b6f* complexes with styrene maleic acid, Biochim. Biophys. Acta - Bioenerg. 1859 (2018) 215–225, https://doi.org/10.1016/j.bbabio.2017.12.005.
[43] S.C.L. Hall, C. Tognoloni, G.J. Price, B. Klumperman, K.J. Edler, T.R. Dafforn, T. Arnold, Influence of poly(styrene-co-maleic acid) copolymer structure on the properties and self-assembly of SMALP nanodiscs, Biomacromolecules 19 (2018) 761–772, https://doi.org/10.1021/acs.biomac.7b01539.
[44] C. Sun, S. Benlekbir, P. Venkatakrishnan, Y. Wang, S. Hong, J. Hosler, E. Tajkhorshid, J.L. Rubinstein, R.B. Gennis, Structure of the alternative complex III in a supercomplex with cytochrome oxidase, Nature 557 (2018) 123–126, https://doi.org/10.1038/s41586-018-0061-y.
[45] S. Scheidelaar, M.C. Koorengevel, C.A. van Walree, J.J. Dominguez, J.M. Dörr, J.A. Killian, Effect of polymer composition and pH on membrane solubilization by styrene-maleic acid copolymers, Biophys. J. 111 (2016) 1974–1986, https://doi.org/10.1016/j.bpj.2016.09.025.
[46] J. Broecker, B.T. Eger, O.P. Ernst, Crystallogenesis of membrane proteins mediated by polymer-bounded lipid nanodiscs, Structure 25 (2017) 384–392, https://doi.org/10.1016/j.str.2016.12.004.
[47] J.M. Dörr, M.C. Koorengevel, M. Schäfer, A.V. Prokofyev, S. Scheidelaar, E.A.W. van der Cruijsen, T.R. Dafforn, M. Baldus, J.A. Killian, Detergent-free isolation, characterization, and functional reconstitution of a tetrameric K^+ channel: the power of native nanodiscs, Proc. Natl. Acad. Sci. 111 (2014) 18607–18612, https://doi.org/10.1073/pnas.1416205112.
[48] M. Tanaka, A. Hosotani, Y. Tachibana, M. Nakano, K. Iwasaki, T. Kawakami, T. Mukai, Preparation and characterization of reconstituted lipid–synthetic polymer discoidal particles, Langmuir 31 (2015) 12719–12726, https://doi.org/10.1021/acs.langmuir.5b03438.
[49] C. Vargas, R.C. Arenas, E. Frotscher, S. Keller, Nanoparticle self-assembly in mixtures of phospholipids with styrene/maleic acid copolymers or fluorinated surfactants, Nanoscale 7 (2015) 20685–20696, https://doi.org/10.1039/C5NR06353A.
[50] D. Olmos, E.V. Martín, J. González-Benito, New molecular-scale information on polystyrene dynamics in PS and PS–$BaTiO_3$ composites from FTIR spectroscopy, Phys. Chem. Chem. Phys. 16 (2014) 24339–24349, https://doi.org/10.1039/C4CP03516J.
[51] K. Nakanishi, Infrared absorption spectroscopy. Practical, second, Holden-Day, Inc., San Francisco and Nankodo Company Limited, Tokyo, San Francisco and Tokyo, 1964.
[52] R.M. Silverstein, F.X. Webster, D.J. Kiemle, Spectrometric Identification of Organic Compounds, John Wiley & Sons, 2005.
[53] Y. Samchenko, O. Korotych, L. Kernosenko, S. Kryklia, O. Litsis, M. Skoryk, T. Poltoratska, N. Pasmurtseva, Stimuli-responsive hybrid porous polymers based on acetals of polyvinyl alcohol and acrylic hydrogels, Colloids Surf. A Physicochem. Eng. Asp. 544 (2018) 91–104, https://doi.org/10.1016/j.colsurfa.2018.02.015.
[54] H.Y. Nakatani, J. Barber, An improved method for isolating chloroplasts retaining their outer membranes, Biochim. Biophys. Acta - Bioenerg. 461 (1977) 510–512, https://doi.org/10.1016/0005-2728(77)90237-7.
[55] K. Cline, Import of proteins into chloroplasts. Membrane integration of a thylakoid precursor protein reconstituted in chloroplast lysates, J. Biol. Chem. 261 (1986) 14804–14810 (accessed September 4, 2018).
[56] K. Sauer, A Role for Manganese in oxygen evolution in photosynthesis, Acc. Chem. Res. 13 (1980) 249–256, https://doi.org/10.1021/ar50152a001.
[57] Y. Umena, K. Kawakami, J.-R. Shen, N. Kamiya, Crystal structure of oxygen-evolving photosystem II at a resolution of 1.9 Å, Nature 473 (2011) 55–60, https://doi.org/10.1038/nature09913.
[58] D.P. Carter, L.A. Staehelin, Proteolysis of chloroplast thylakoid membranes. II. Evidence for the involvement of the light-harvesting chlorophyll ab-protein complex in thylakoid stacking and for effects of magnesium ions on photosystem II-light-harvesting complex aggregates in the absence of membrane stacking, Arch. Biochem. Biophys. 200 (1980) 374–386, https://doi.org/10.1016/0003-9861(80)90367-7.
[59] H. Kirchhoff, W. Haase, S. Haferkamp, T. Schott, M. Borinski, U. Kubitscheck, M. Rögner, Structural and functional self-organization of Photosystem II in grana thylakoids, Biochim. Biophys. Acta - Bioenerg. 1767 (2007) 1180–1188, https://doi.org/10.1016/J.BBABIO.2007.05.009.
[60] I. Rumak, K. Gieczewska, B. Kierdaszuk, W.I. Gruszecki, A. Mostowska, R. Mazur, M. Garstka, 3-D modelling of chloroplast structure under (Mg_{2+}) magnesium ion treatment. Relationship between thylakoid membrane arrangement and stacking, Biochim. Biophys. Acta - Bioenerg. 1797 (2010) 1736–1748, https://doi.org/10.1016/J.BBABIO.2010.07.001.
[61] J.J. Lamb, G. Røkke, M.F. Hohmann-Marriott, Chlorophyll fluorescence emission spectroscopy of oxygenic organisms at 77 K, Photosynthetica. 56 (2018) 105–124, https://doi.org/10.1007/s11099-018-0791-y.